SPECTROSCOPIC STUDIES OF IONIC INTERACTIONS AND COMPLEXATION OF ALKALI METAL IONS IN VARIOUS SOLVENTS

Dissertation for the Degree of Ph. D.
MICHIGAN STATE UNIVERSITY
YVES M. CAHEN
1975

THESIS

Michigan State University

This is to certify that the

thesis entitled

Spectroscopic Studies of Ionic Interactions and Complexation of Alkali Metal Ions in Various Solvents

presented by

Yves M. Cahen

has been accepted towards fulfillment of the requirements for

Ph.D. degree in Chemistry

Major professor

Date February 25, 1975

O-7639

BINDING BY HOAG & SONS' BOOK BINDERY INC. LIBRARY BINDERS SPRINGPORT, MICHIGAN

ABSTRACT

SPECTROSCOPIC STUDIES OF IONIC INTERACTIONS AND COMPLEXATION OF ALKALI METAL IONS IN VARIOUS SOLVENTS

By

Yves M. Cahen

Chemical shifts of lithium-7 nucleus were measured in eleven nonaqueous solvents against 4.0 M aqueous lithium perchlorate solution. Lithium perchlorate, chloride, bromide, iodide, triiodide and tetraphenylborate were used. The shifts ranged from +2.80 ppm for acetonitrile, down to -2.54 ppm for pyridine. In dimethylsulfoxide and dimethylformamide no evidence for contact ion pairing was observed. Formation of contact ion pairs was particularly evident in tetrahydrofuran, nitromethane and tetramethylguanidine. The large broadening of the ^{35}Cl resonance of the perchlorate ion in these solvents is in agreement with the above explanation. In contrast to sodium-23 NMR, no correlation was found between limiting chemical shifts in different solvents and the Gutmann donor numbers of these solvents.

Formation constants of lithium ion complexes with 1,5-polymethylenetetrazoles and 3,3-disubstituted glutarimides have been determined in nitromethane solutions by lithium-7

NMR. Concentration dependence of the obtained values are explained by the competitive ion pair formation. Glutarimide complexes were found to be somewhat more stable than the pentamethylenetetrazole complexes.

Lithium-7 NMR studies were performed on lithium ion complexes with cryptands C222, C221 and C211 in water and in several nonaqueous solvents. In the case of the first two cryptands the exchange between the free and complexed lithium ion was fast by the NMR time scale and only one population-average resonance was observed. Cryptand 211 forms much more stable lithium complexes and two ^{7}Li resonances (corresponding to the free and the bound Li^{+}) were observed for solutions containing excess of the Li^{+} ion. The limiting chemical shifts of the complex were found to be independent of the solvent indicating that the lithium ion is completely shielded by the cryptand. Formation constants of lithium-C222 complexes were determined in water and pyridine solutions. The values obtained were: $\log K_{H_2O} = 0.99 \pm 0.15$ and $\log K_{Py} = 2.94 \pm 0.10$.

The kinetics of complexation reactions of the lithium ion with cryptand C211 in pyridine, water, dimethylsulfoxide, dimethylformamide and formamide and with cryptand C221 in pyridine were investigated by temperature dependent ^{7}Li NMR. The energies of activation for the release of Li^{+} from Li^{+}-C211 complexes increase with the increasing donicity of the solvent as expressed by the Gutmann donor number. The transition state of the complexation reaction

must involve substantial ionic solvation. Using the formation constant of the Li^+-C211 cryptate in water, the rate constant for the forward reaction was found to be $k_f = 0.98 \times 10^3$ sec.

Far infrared spectra of sodium and lithium cryptates were observed in several nonaqueous solvents. The spectra are characterized by a broad band whose frequency is independent of the solvent or of the anion and which is assigned to the vibration of the cation in the cryptand cavity. The band frequencies were 234 ± 2, 218 ± 1, 234 ± 3 and 348 ± 1 cm^{-1} for Na^+-C222, Na^+-C221, Li^+-C221 and Li^+-C211 cryptates respectively. These bands were found to be Raman-inactive, indicating that the cation-ligand interaction is very largely electrostatic in nature.

SPECTROSCOPIC STUDIES OF IONIC INTERACTIONS AND COMPLEXATION OF ALKALI METAL IONS IN VARIOUS SOLVENTS

By

Yves M. Cahen

A DISSERTATION

Submitted to

Michigan State University

in partial fulfillment of the requirements

for the degree of

DOCTOR OF PHILOSOPHY

Department of Chemistry

1975

ACKNOWLEDGMENTS

The author wishes to express his sincere gratitude to Professor Alexander I. Popov for his guidance, encouragement and friendship throughout this study, Professor Bernard Tremillon of "Ecole Nationale Superieure de Chimie de Paris" and Dr. Richard Combes for their introduction to research and their friendship.

Professor James L. Dye is acknowledged for his helpful suggestions and discussions as second reader.

Gratitude is also extended to the Department of Chemistry, Michigan State University, and the National Science Foundation for financial aid.

Special thanks are given to Dr. Richard Bodner and Dr. Mark S. Greenberg for numerous enlightening discussions and their help during the early part of this work, to the former and present members of the group for their constant moral support, to Joe Ceraso for his constant help throughout the kinetic part of this work, to Wayne DeWitte for his expenditure of time in proofreading this thesis, to Messrs.Eric T. Roach and Frank Bennis, without whose cooperation the NMR investigations would have been much more difficult, to the friends in Michigan and elsewhere who contributed to render our stay in America a wonderful and unique experience.

Deep gratitude to our families for their encouragement, abundant mail and numerous visits.

Deep appreciation to my wife, Yvette, for her love, patience and encouragement throughout the years of graduate study.

To her and to our families, I dedicate this thesis.

TABLE OF CONTENTS

Chapter Page

LIST OF TABLES. vii

LIST OF FIGURES ix

LIST OF NOMENCLATURE, ABBREVIATIONS AND SYMBOLS . . .xiv

I HISTORICAL

A. SPECTROSCOPIC STUDY OF SOLVATION AND IONIC ASSOCIATION. 1

1. Introduction 1

2. Vibrational Spectroscopy 1

3. Nuclear Magnetic Resonance 3

B. COMPLEXATION OF ALKALI METAL IONS BY ORGANIC LIGANDS. 9

1. Tetrazoles and Glutarimides. . . . . .

2. Crowns and Cryptands 10

II EXPERIMENTAL PART

A. SALTS. 20

B. LIGANDS. 20

C. SOLVENTS 21

D. SAMPLE PREPARATION 22

E. INSTRUMENTAL MEASUREMENTS. 24

1. Lithium-7 NMR. 24

2. Chlorine-35 NMR. 25

3. Infrared Spectra 26

4. Laser Raman Spectra. 26

5. Data Handling. 27

III SPECTROSCOPIC STUDIES OF IONIC SOLVATION BY LITHIUM-7 NMR, CHLORINE-35 NMR AND RAMAN SPECTROSCOPY

A. INTRODUCTION 28

B. RESULTS AND DISCUSSION 28

Chapter Page

IV SPECTROSCOPIC STUDIES OF COMPLEXATION OF ALKALI METAL IONS

I. LITHIUM-7 NMR STUDY OF THE Li^+ COMPLEXES WITH CONVULSANT POLYMETHYLENE TETRAZOLES AND GLUTARIMIDES IN NITROMETHANE SOLUTIONS. . 52

A. INTRODUCTION. 52

B. RESULTS AND DISCUSSION. 53

II. STUDY OF THE COMPLEXATION OF ALKALI METAL IONS BY CRYPTAND LIGANDS IN VARIOUS SOLVENTS. 60

A. LITHIUM-7 NMR STUDY 60

1. Lithium-7 Chemical Shift of Lithium-222, 221, 211 Cryptates in Various Solvents. 60

2. Lithium NMR Study of the Lithium Ion-Lithium Cryptate Exchange in Various Solvents. 70

B. FAR INFRARED AND RAMAN STUDY OF LITHIUM AND SODIUM CRYPTATES IN NONAQUEOUS SOLVENTS. 88

1. Introduction. 88

2. Results and Discussion. 88

C. CONCLUSIONS AND SUGGESTIONS FOR FURTHER STUDIES 101

APPENDICES

I LITHIUM-7 CHEMICAL SHIFTS VS 4.0 M AQUEOUS $LiClO_4$ OF VARIOUS LITHIUM SALTS IN VARIOUS SOLVENTS. 103

II DETERMINATION OF COMPLEX FORMATION CONSTANTS BY THE NMR TECHNIQUE, DESCRIPTION OF COMPUTER PROGRAM KINFIT AND SUBROUTINE EQN 113

III NMR LINE SHAPE ANALYSIS FOR TWO SITE EXCHANGE. DESCRIPTION OF COMPUTER PROGRAM AND SUB-ROUTINE EQN 118

A. NMR LINE SHAPE ANALYSIS FOR TWO SITE EXCHANGE. 118

Chapter Page

B. DETERMINATION OF τ VALUES FROM LINE SHAPE ANALYSIS OF AN NMR SPECTRUM AT A GIVEN TEMPERATURE. DESCRIPTION OF COMPUTER PROGRAM AND SUBROUTINE EQN. 128

C. DETERMINATION OF THE ACTIVATION ENERGY (E_a). DESCRIPTION OF THE COMPUTER PROGRAM AND SUBROUTINE 129

LITERATURE CITED. 133

LIST OF TABLES

Table		Page
I	Donor Number (DN) and Dielectric Constant (ε) of Some Important Solvents (38).	6
II	Key Solvent Properties and Correction for Magnetic Susceptibility on DA-60	23
III	Limiting Chemical Shifts of ^{7}Li (0.02 M LiI_3) in Various Solvents.	34
IV	Line Broadening of ^{35}Cl Resonance in $LiClO_4$ Solutions	40
V	Formation Constants of Li^+-Tetrazole and Li^+-Glutarimide Complexes	57
VI	^{7}Li-NMR Study of C222, C221, C211, Lithium Complexes in Various Solvents at Room Temperature.	61
VII	^{7}Li Chemical Shifts as a Function of Ligand/Li^+ Mole Ratio for the Determination of the Formation Constants of Li^+-C222 Complexes in Water and Pyridine	68
VIII	Description of $\Delta(\delta)$ as a Function of Temperature.	81
IX	Exchange Rates and Thermodynamic Parameters of Lithium Cryptate Exchange in Various Solvents.	84
X	Far Infrared Bands of Sodium and Lithium Salts in Various Solvents.	92

Table		Page
XI	Frequencies (cm^{-1}) of the Major Far Infrared Bands for Cryptates in Various Solvents.	94
XII	Raman Bands of Li^{+}-C211 Complexes in Pyridine and Nitromethane Solutions	100

LIST OF FIGURES

Figure		Page
1	Structure of (A) 1,5-cyclopoly-methylenetetrazoles, and (B) 3,3-disubstituted glutarimides	10
2	Dibenzo-18-crown-6. The number 6 refers to the total number of oxygens and 18 to the total number of atoms in the poly-ether ring	11
3	Cryptand 222, 221, 211 and their cavity diameter (Å)	15
4	Exo-exo, endo-endo and exo-endo conformations of 222 cryptate	16
5	Structure of (A) "proton" cryptate and (B) "silver" cryptate.	18
6	^{7}Li chemical shifts of lithium salts in propylene carbonate and dimethyl-formamide.	30
7	^{7}Li chemical shifts of lithium salts in dimethylsulfoxide and methanol.	31
8	^{7}Li chemical shifts of lithium salts in tetrahydrofuran	32
9	^{7}Li chemical shifts of lithium salts in acetonitrile and nitromethane	33
10	^{7}Li chemical shift of lithium salts in acetic acid and tetramethyl-guanidine.	38

Figure		Page
11	^{7}Li chemical shift and ^{35}Cl NMR resonance line width of $LiClO_4$ in nitromethane as a function of lithium concentration	46
12	Raman spectra of ClO_4^- 935 cm^{-1} band as a function of $LiClO_4$ concentration in nitromethane.	49
13	Raman spectra of the ClO_4^- 935 cm^{-1} band as a function of $LiClO_4$ concentration in, (A) methanol, (B) tetramethylguanidine, (C) acetonitrile	50
14	Plot of ^{7}Li chemical shift with reference to 4.0 M aqueous $LiClO_4$ vs mole ratio of 3,3-dimethyl glutarimide to Li^+ at constant $[Li^+]$ = 0.100 M. Solid line is computer-generated curve and dots are the experimental points	56
15	Plot of formation constants vs lithium ion concentration. A - Glutarimide. B - 3-ethyl-3-methyl glutarimide. C - Pentamethylenetetrazole.	59
16	Lithium-7 NMR spectra of lithium-C211 cryptate in various solvents; [C211] = 0.25 M, $[Li^+]$ = 0.50 M. Chemical shift of Li^+-C211 is at 0.41 ppm vs aqueous $LiClO_4$ solution at infinite dilution.	64

Figure		Page
17	Plot of ^{7}Li chemical shift with reference to 4.0 M aqueous $LiClO_4$ vs mole ratio of cryptand 222 to Li^+ at constant $[Li^+]$ = 0.25 M. Solid line is computer-generated curve and dots are experimental points	69
18	Lithium-7 NMR spectra of 0.50 M $LiClO_4$, 0.25 M C211 solution in pyridine at various temperatures	73
19	Lithium-7 NMR spectra of 0.50 M $LiClO_4$, 0.25 M C211 solution in formamide at various temperatures.	74
20	Lithium-7 NMR spectra of 0.50 M $LiClO_4$, 0.25 M C211 solution in dimethylformamide at various temperatures	75
21	Lithium-7 NMR spectra 0.50 M $LiClO_4$, 0.25 M C211 solution in dimethylsulfoxide at various temperatures.	76
22	Lithium-7 NMR spectra of 0.50 M LiI, 0.25 M C211 solution in water at various temperatures.	77
23	Lithium-7 NMR spectra of 0.50 M $LiClO_4$, 0.25 M C221 solution in pyridine at various temperatures	78

Figure		Page
24	Computer fit of spectra obtained with 0.50 M $LiClO_4$, 0.25 M C211 in formamide at 143.3°C. X means an experimental point, 0 means a calculated point, = means an experimental and calculated point are the same within the resolution of the plot	80
25	Log k_b vs 1/T plot for 0.50 M $LiClO_4$, 0.25 M C211 in (A) pyridine, (B) formamide, (C) dimethylformamide, (D) dimethylsulfoxide, (E) 0.50 M LiI, 0.25 M C211 in water, and (F) 0.50 M $LiClO_4$, 0.25 M C221 in pyridine.	83
26	Schematic representation of the complexation of lithium ion by cryptands 211 and 221. S_1 represents a good donor solvent, S_2 a poor one	87
27	Far infrared spectra of nitromethane, pyridine and DMSO solutions of Na^+X^- salts (X^- = BPh_4^- and I^-) (solid lines) and of analogous 222 cryptates (dashed lines)	90
28	Far infrared spectra of nitromethane, pyridine and acetonitrile solutions of Li^+X^- salts (X^- = ClO_4^- and I^-) (solid lines) and of analogous 211 cryptates (dashed lines)	91

Figure Page

29 Raman and far infrared spectra of ^{6}Li-C211 and ^{7}Li-C211 cryptates in nitromethane solution. S-solvent band. 96

30 Comparison of ion motion band frequencies for sodium and lithium salts and their 222 and 211 cryptates respectively in pyridine, acetonitrile, nitromethane, dimethylsulfoxide solutions 98

LIST OF NOMENCLATURE, ABBREVIATIONS AND SYMBOLS

Contact Ion Pairs. Pairs of ions, linked electrostatically, but with no covalent bonding between them.

Solvent Shared Ion Pairs. Pairs of ions, linked electrostatically by a single, oriented solvent molecule.

Solvent Separated Ion Pairs. Pairs of ions, linked electrostatically but separated by more than one solvent molecule.

CH_3CN : Acetonitrile

DMF : N,N-Dimethylformamide

DMSO : Dimethylsulfoxide

PC : Propylene Carbonate

THF : Tetrahydrofuran

TMG : 1,1,3,3-Tetramethylguanidine

CH_3NO_2 : Nitromethane

MeOH : Methanol

C222 : Cryptand 222 ($C_{18}H_{36}N_2O_6$) MW = 376.5 g

C221 : Cryptand 221 ($C_{16}H_{32}N_2O_5$) MW = 332.4 g

C211 : Cryptand 211 ($C_{14}H_{28}N_2O_4$) MW = 288.4 g

CHAPTER I

HISTORICAL PART

A. SPECTROSCOPIC STUDY OF SOLVATION AND IONIC ASSOCIATION

1. Introduction

Alkali metal ions and their salts play an important role in chemistry as well as in biological processes. However, their solution chemistry, especially in nonaqueous solvents, still remains largely unknown. For example, we have only a very imperfect knowledge of the exact nature of the chemical species present in such solutions, of the equilibria between them, and of the role of the solvent in these equilibria.

Classical techniques such as conductance are still used for characterization of ionic equilibria in solutions, either alone (1-4) or in combination with ultrasonic relaxation (5). Recently spectroscopic techniques have been shown to be very useful tools for such investigations. They are now extensively used to obtain qualitative information about the kinds of interactions which are predominant in solutions (solvent-solvent, solvent-solute, solute-solute interactions) as well as quantitative data about equilibria in solution (ion pair formation, complexation, kinetics of complexation).

2. Vibrational Spectroscopy

Evans and Lo (6) studied far infrared spectra of tetrapentyl- and tetrabutylammonium chlorides and bromides in benzene solutions, and observed bands which could not be

attributed to a vibrational mode of either the solute or the solvent. They concluded that these bands were due to cation-anion ion pair vibration in solution. At the same time Edgell et al. (7-8) likewise reported ion pair vibration bands in cobalt tetracarbonyl and manganese pentacarbonyl solutions in tetrahydrofuran. Popov and coworkers (9-17) extended these far infrared studies to a wide range of nonaqueous media. They found that in solvents of high solvating ability, such as dimethylsulfoxide or 1-methyl-2-pyrrolidone, new far infrared bands were observed whose frequencies were dependent on the solvent and on the cation but were not affected by a change in the counter ion, thus representing vibration of a cation in a solvent cage ("solvation bands"). In solvents of medium and low donor ability the frequencies of such bands were occasionally anion-dependent. In these cases the anion penetrates the first solvation shell of the cation forming contact ion pairs.

Tsatsas and Risen (18) observed far infrared bands for lithium and calcium ions in ethylene methacrylate ionic polymers. Recently, Edgell and coworkers (19) examined the infrared spectrum of thallium tetracarbonylcobaltate in several solvents as a function of temperature. Only a single ion site was found in dimethylformamide, dichloroethane and dimethylsulfoxide solutions. Several kinds of sites were found in tetrahydrofuran, acetonitrile and nitromethane solution, including free ions, solvent

separated ion pairs, contact ion pairs and triple ions. Barriol et al., (20) tried to calculate the frequency shift attributed to the solvent effect on an infrared band using the classical model of an anharmonic oscillator centered in the Onsager cavity.

Corset et al. (21-22) and Popov and coworkers (13) studied preferential solvation of the lithium ion in binary solvent mixtures (acetone, nitromethane). Recently Baum and Popov (23), extended the earlier work and used Raman spectroscopy, infrared spectroscopy, lithium-7 NMR, and chlorine-35 NMR to study Li^+ ion solvation in acetone-nitromethane mixtures. They found that Li^+ ion is solvated by four acetone molecules and calculated equilibrium constant values for the stepwise solvation reaction.

3. Nuclear Magnetic Resonance

Nuclear magnetic resonance (NMR) has become a powerful tool for the investigation of electrolyte solutions and of complexation reactions. The chemical shifts and line widths of the nuclear resonances of various nuclei can yield information about ion-ion, ion-solvent and ion-ligand interaction. There have been many studies of solvent molecules or the solvated species by proton NMR, some typical examples can be found in References (24) to (27). However, relatively few studies of the magnetic resonances of nuclei other than protons have been reported.

All the alkali metal and halide ions possess at least

one isotope with a magnetic nucleus, i.e., ^{7}Li, ^{23}Na, ^{39}K, ^{87}Rb, ^{133}Cs, ^{19}F, ^{35}Cl, $^{79,81}Br$ and ^{127}I. Deverell and Richards (28) studied the chemical shifts of ^{23}Na, ^{39}K, ^{87}Rb and ^{133}Cs nuclei in aqueous solutions of alkali halides and nitrates as a function of salt concentration. The concentration dependences of the chemical shifts were attributed to interactions between the cations and anions in solutions. Recent use of high resolution NMR pulse Fourier transform techniques (29-30) has made possible the investigation of nuclei with low magnetic moment or low natural abundance.

The exact nature of the chemical shift is not completely understood at this time. The chemical shift arises from the fact that a magnetic nucleus may experience local magnetic fields. Such magnetic fields are due to the surrounding electronic motion as modified by chemical bonding and molecular association. Atomic chemical shifts may be considered to be a sum of diamagnetic term (σ_d) arising from the inner symmetrical electrons which set up a small magnetic field opposed to the large, externally applied field, and a paramagnetic term (σ_p) arising from non-spherically symmetrical valence electron orbitals which restrict electronic motions. Jameson and Gutowsky (31) have discussed the apparent increase in observed chemical shift with increasing atomic number and pointed out that the diamagnetic contribution to the chemical shift can be calculated and that the often predominant paramagnetic

contribution is difficult to estimate.

The chemical shift of ^{23}Na is dominated by the paramagnetic contribution. The range of chemical shifts observed is rather large, and the large quadrupole moment of the nucleus renders this nucleus a sensitive probe of the neighboring electronic environment. Sodium-23 NMR has been recently used to study nonaqueous electrolyte solutions. Popov and coworkers observed the chemical shifts of various sodium salts in neat and mixed nonaqueous solvents (32-36). They were able to identify contact ion pair formation and found an upfield change of the ^{23}Na chemical shift with increasing concentration of sodium perchlorate solutions in various solvents. Similar results were obtained by Van Geet and Templeman for aqueous perchlorate solutions (37). Popov *et al.* also observed a linear relationship between Gutmann donor numbers* (38) of various nonaqueous solvents and the ^{23}Na chemical shifts (at infinite dilution) in those solvents (39).

By monitoring the ^{23}Na chemical shift as a function of the amount of water added, Van Geet (40) determined that the hydration number of the sodium ion is between three and four.

---

*Gutmann's donor number (38) is the enthalpy of complex formation between the given solvent and antimony pentachloride in 1,2-dichloroethane solution:

$$S + SbCl_5 \xrightarrow{1,2\text{-DCE}} S.SbCl_5$$

Gutmann used the term "donicity" when referring to the donor ability of a solvent. Donor numbers of some important solvents are given in Table I.

Table I. Donor number (DN) and dielectric constant (ε) of some important solvents (38).

Solvent	DN	ε
1,2-dichloroethane	----	10.1
Nitromethane	2.7	10.0
Nitrobenzene	4.4	34.8
Acetic anhydride	10.5	20.7
Benzonitrile	11.9	25.2
Acetonitrile	14.1	38.0
Sulpholane	14.8	42.0
Propionitrile	16.1	27.7
Ethylene carbonate	16.4	89.1
Acetone	17.0	20.7
Ethyl acetate	17.1	6.0
Tetrahydrofuran (THF)	20.0	7.6
Dimethylformamide (DMF)	26.6	36.1
Dimethylsulfoxide (DMSO)	29.8	45.0
Pyridine	33.1	12.3
Hexamethylphosphoramide	38.2	30.0
Water	18.0 (33.0[a])	81.0

[a]Predicted by ^{23}Na NMR (39).

Unlike sodium, the paramagnetic contribution to the ^{7}Li chemical shift is small enough to cause the diamagnetic contribution to be equally important. Akitt and Downs (41) pointed out that the lithium nucleus should be highly suitable as a nuclear magnetic resonance probe because of its high sensitivity, enhanced by an exceptionally narrow line width for ionic solutions. Consequently, very accurate measurements of chemical shifts are possible. Lithium-7, and lithium-6 NMR techniques were used by Attalla and Eckstein to determine the isotopic ratios in isotopic mixtures (42). In an early work Graig and Richards (43) did not observe any significant differences in ^{7}Li chemical shifts of lithium chloride in different solvents or at varying salt concentration. The negative results are probably due to the inaccuracy of their measurements. Maciel et al. (44) and Akitt and Downs (41) measured the ^{7}Li chemical shifts of solutions of lithium bromide and perchlorate in water and in eleven organic solvents and observed that the frequency of the ^{7}Li resonance is indeed sensitive to the environment. Recently Cox et al. (45-46) studied the ^{7}Li nuclear magnetic resonance of some aromatic ion pairs in various solvents. They discussed their results in terms of the type of ion pairs formed in solution and the possible structures of these ion pairs (46).

Both ^{23}Na NMR and ^{7}Li NMR have been found useful for the determination of formation constants of weak complexes (47-48). It is clear that ^{7}Li NMR may provide useful

information concerning the presence and types of interactions in electrolyte solutions and can also be a tool for the investigation of complexation reactions. A more extensive historical and theoretical discussion on ^{7}Li NMR can be found in the Ph.D. thesis of P. R. Handy (49).

To complement alkali metal cation NMR, nuclear magnetic resonance of anions can also provide information on electrolyte solutions. Dodgen et al. (50) reported that the ^{35}Cl chemical shift of $HClO_4$ was -946±6 ppm from concentrated aqueous HCl solution, with a linewidth of 62.5 Hz. The same chemical shift was observed by Saito (51). In this case, however, the linewidth was found to be only 42 Hz. Richards et al., (52) studied chemical shifts and transverse nuclear relaxation times of ^{35}Cl and ^{81}Br in aqueous-methanol solutions of LiCl and LiBr. They observed that most of the line broadening is due to changes in the viscosity of the solutions with concentration. Langford and Stengle (53) studied the solvation of the chloride ion by ^{35}Cl NMR in mixtures of acetonitrile and dimethylsulfoxide with water. They observed that a nearly equivalent competition by the two solvents for the Cl^- ion solvation sites occurs in both mixtures and that the immediate environment of Cl^- is related to the long-range structural aspects of the solvent mixtures.

Deverell and Richards (54) surveyed the chemical shifts of ^{35}Cl, ^{81}Br and ^{127}I nuclei in aqueous solutions of alkali halides and postulated that direct cation-anion

collisions were the predominant cause of the concentration dependence of the observed chemical shifts of potassium, rubidium and cesium halide salts. For lithium and sodium halide solutions they found that the ionic interactions were of prime importance for the determination of the chemical shift of the halogen. Recently, Hall (55) pointed out that halogen NMR can be a useful tool for the investigation of biochemical and biophysical processes and systems. Langford and coworkers (56) reported results on solvent and counterion dependence of $^{19}F^-$ chemical shifts. The collision processes concept allowed them to separate the large effect arising from collisions and the primary solvation sphere from the smaller effects of outer sphere interactions.

B. COMPLEXATION OF ALKALI METAL IONS BY ORGANIC LIGANDS

1. Tetrazoles and Glutarimides

Compounds such as 1,5-cyclopolymethylenetetrazoles (Figure 1A) and 3,3-disubstituted glutarimides (Figure 1B) are characterized by their strong stimulating action on the central nervous system. For example, the convulsant activity of polymethylenetetrazoles increases with increasing length of the polymethylene chain (57-58). Popov *et al.* (59) investigated donor properties of tetrazoles in 1,2-dichloroethane by spectrophotometric measurements. They did not observe a correlation between the length of the hydrocarbon chain and the stability of the iodine complex.

Complexing ability with alkali metal ions could be an important factor in the physiological activity of these compounds, if such molecules act as ionic carriers through the membranes of neural synapses. Alkali metal NMR has been used for the determination of formation constants of complexes of pentamethylenetetrazole with sodium (48) and lithium (47) in nitromethane, however more work is needed to determine whether or not convulsant activity of these drugs is due to their ability to complex alkali metal ions.

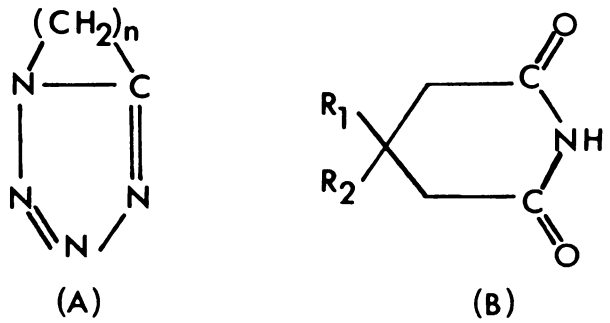

Figure 1. Structure of (A) 1,5-cyclopolymethylenetetrazoles, and (B) 3,3-disubstituted glutarimides.

2. Crowns and Cryptands

In recent years, macrocyclic polyethers have been synthesized which have a remarkable ability to form very stable complexes with alkali metal cations. Not only do these compounds present considerable interest from a purely chemical point of view, but they can serve as models in simulating the processes which govern ion-transport through membranes

in biological systems (60).

Cyclic polyethers, or "crown" ethers, developed by Pedersen (61), were the first such complexing agents to appear. A typical "crown" is shown in Figure 2

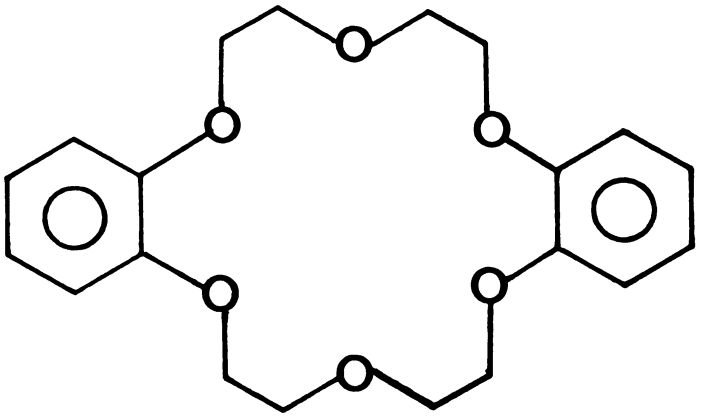

Figure 2. Dibenzo-18-crown-6. The number 6 refers to the total number of oxygens and 18 to the total number of atoms in the polyether ring.

Truter et al., determined the crystal structures of sodium dibenzo-18-crown-6 (62), potassium dibenzo-30-crown-10 (62), and potassium benzo-15-crown-5 (63). They showed that in the solid state, the alkali metal ion is located in the middle of the polyether ring. In solution, crowns are also likely to form a bidimensional complex where the cation lies in the center of the polyether ring. Pedersen (61) studied crown complexes in solution by proton NMR and vibrational spectroscopy. He measured the solubility of dibenzo-18-crown-6-K^+ salts in seventeen nonaqueous solvents and

pointed out that the saturated cyclic polyethers have the useful property of solubilizing salts in aprotic solvents. Dye et al. (64) using this property, reported a new technique for dissolving alkali metals in solvents, such as ethers, in which they are ordinarily either insoluble or only slightly soluble.

Pedersen (65) found that crowns do not necessarily form only one to one complexes with metal ions. Thus with dicyclo-18-crown-6, in addition to the 1:1 complexes, he also obtained 2:1 complexes, e.g., dibenzo-18-crown-6-K^+, and 3:2 complexes e.g., dibenzo-18-crown-6-Cs^+. The 2:1 and 3:2 complexes may have a "sandwich" structure.

Further work by Pedersen (66) showed that dicyclohexyl-15-crown-5 is the best complexing agent of the crown type for Na^+ ion; on the other hand, dicyclohexyl-16-crown-5, is the most specific crown for Na^+ as compared with other alkali cations. Frensdorff obtained formation constants of crown complexes in aqueous and methanolic solution by potentiometry (67), and in chloroform by picrate extractions (68). Risen et al. (69) made an interesting far infrared study of dibenzo-18-crown-6 complexes of sodium and potassium. They found a cation dependent band at 167 cm^{-1} for potassium and 213 cm^{-1} for sodium. This vibration is due to the crown-encaged cation and is solvent and cation independent.

Shchori et al. (70) monitored the complexation of sodium ion by dibenzo-18-crown-6 in dimethylformamide by

using ^{23}Na NMR measurements. They were unable to observe two peaks because the line width of the complexed Na^+ ion was very broad, although the line shape analysis indicated that exchange was slow. They reported an activation energy of 12.5 kcal. $mole^{-1}$. Wong, Konizer and Smid (71) studied these systems by using proton NMR with several etheral solvents and pyridine. They observed two sets of ligand protons, one set corresponding to complexed crown and the other to uncomplexed crown. The spectra were analyzed at the coalescence temperature, and results were obtained consistent with those of Shchori et al. (70).

Pedersen and Frensdorff (72) noted that very few data are available on complexation reactions in solvents less polar than methanol, where ion-pair formation becomes significant so that anion effects would be appreciable. Smid et al. (73) investigated the interactions of alkali metal ions and their fluorenyl ion pairs with crown ethers in THF. They concluded that crown ether complexes represent convenient systems to study ion or ion-pair interactions with neutral molecules in both aqueous and nonaqueous media.

The mechanism of complexation reaction of the crown ethers was investigated by Chock (74). Enthalpy of hydration involved in the desolvation step and the binding energy for a given ligand were found to be the two most important factors in the mechanism of complexation and the stability of the resulting complex. These results are in agreement

with the work of Cussler et al. (75), who precisely measured conductances of sodium, potassium and cesium salts in methanol and acetonitrile solutions containing cyclic polyethers (dibenzo-18-crown-6), and obtained the association constants of the respective complexes. They also observed that dibenzo-18-crown-6 complexes selectively sodium as compared to potassium in methanol but in acetonitrile it complexes both cations evenly; thus the observed selectivity is not only a function of the ionic size of the complexed ligand but also of the solvent used. Recently Simmons et al. (76) published an interesting paper about the application of crowns in substitution reactions using potassium hydroxide complexes of dicyclo-18-crown-6. The complexation of the cation enhances the reactivity of the anion (OH^-).

At the height of the interest in crown ethers, Lehn and coworkers (77-78) introduced a new class of complexing agents: diaza-polyoxamacrocycles and macrobicycles called cryptands.

Cryptands are bicyclic molecules in which the length of the ether bridges may be changed to vary the size of the cavity inside the cryptand to accommodate different cations. The word cryptand refers to the ligand and cryptate to the complex. Cryptand 222, 221, 211 are shown in Figure 3.

Like crowns, cryptands have aroused the interest of biologists as carriers in ion selective membranes (79). Their

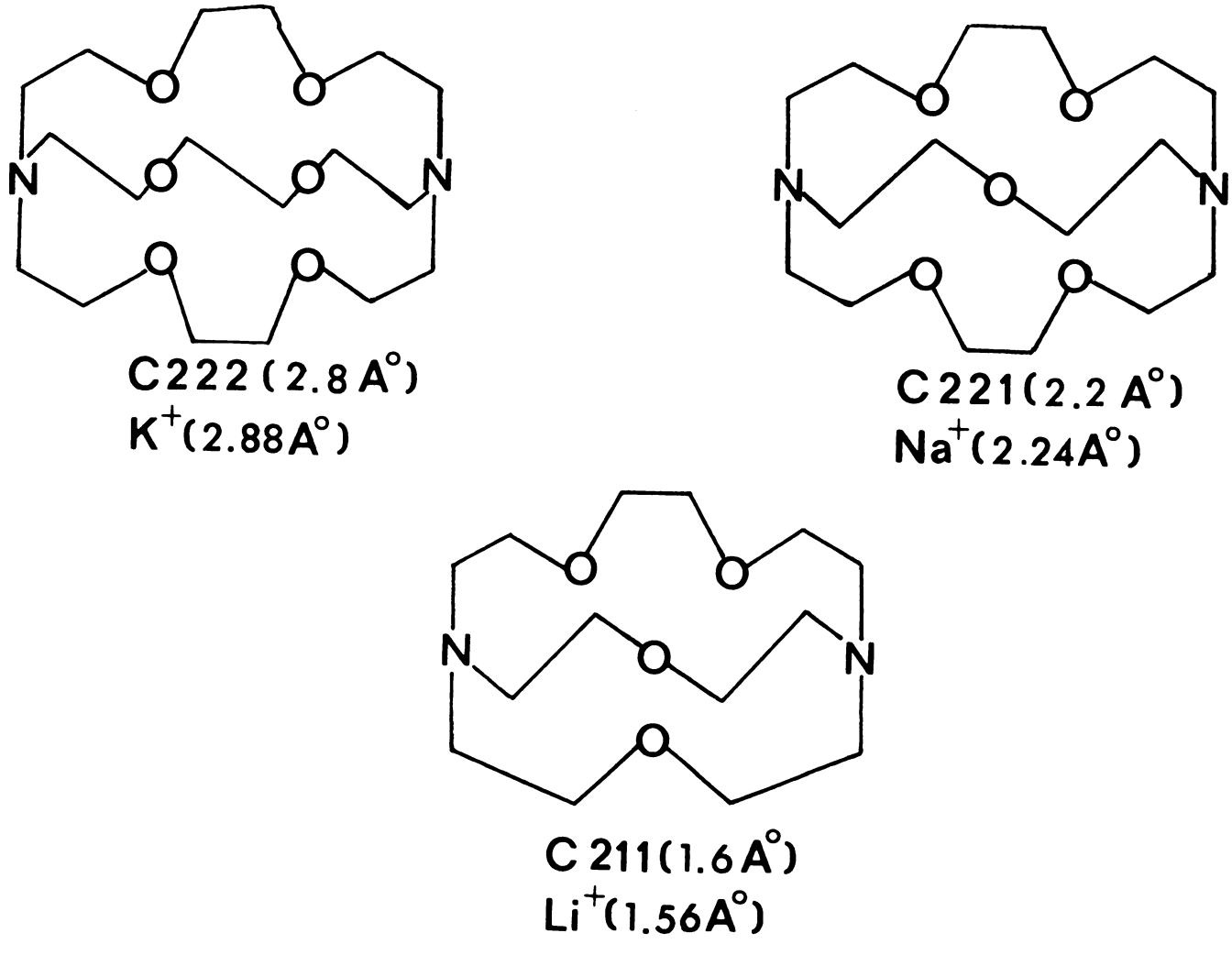

Figure 3. Cryptand 222, 221, 211 and their cavity diameter (Å).

synthesis is complex and time consuming. Important steps involved in the synthesis have already been described by Lehn and coworkers (78-80). Dye et al. (81) made a very important modification in the synthesis by substituting a flow technique for the high dilution steps for cyclization reactions.

Crystal structures of a number of cryptates were determined by Wiess and coworkers, for example silver cryptate (82), cesium and rubidium cryptates (83), potassium cryptate (84), sodium cryptate (85) and lithium cryptate (86). In solution, several conformations may be imagined for cryptates and cryptands, as shown in Figure 4 for cryptate 222. Similar behavior is observed for bicycloalkanes (87) and diazabicycloalkanes (88,89) compounds.

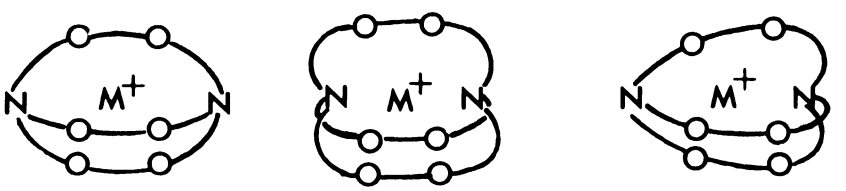

exo-exo endo-endo exo-endo

Figure 4. Exo-exo, endo-endo and exo-endo conformations of 222 cryptate.

However, cryptate complexes have an endo-endo conformation which allows the formation of the suitable cavity and in which the two amine groups can stabilize the complex.

The stability of the cryptate complexes depends to a large extent on the size relationship between the tridimensional cavity of the cryptand and the diameter of the desolvated ion. Figure 3 shows, for example, that C211 is the specific cryptand for Li^+ ion and C222 for K^+.

In the case of weaker complexes, for example Li^+ -C222 cryptates, the solvating ability of the solvent used may play an important role in the complexation reaction. Formation constants have been determined by potentiometric titrations for a very small number of complexes, and only in aqueous and methanolic solutions (80,90).

Directly related to strength of the complexes is the selectivity of the ligand. The synthesis of numerous types of cryptands to match the size of a given cation has been performed by varying the length and the nature of the bridges. For example, C111 which is the specific cryptand for the proton (91) while rubidium cryptate, with a cavity of 6 Å (92) matches the size of the rubidium or silver ions, are shown in Figures 5A and 5B, respectively. Replacement of hydrogen atoms of the bridges by N-R or N-COOR groups to modify the selectivity between "hard" cations (Li^+, Na^+, K^+, . . .) and "soft" cations (Tl^+, Ag^+, Hg^+, Cd^{2+}, . . .) (93) has also been found useful. Bivalent-monovalent cation selectivity was investigated by Lehn et al. (94) for Na^+, K^+ and Ba^{2+} in methanol and water solutions with various cryptands.

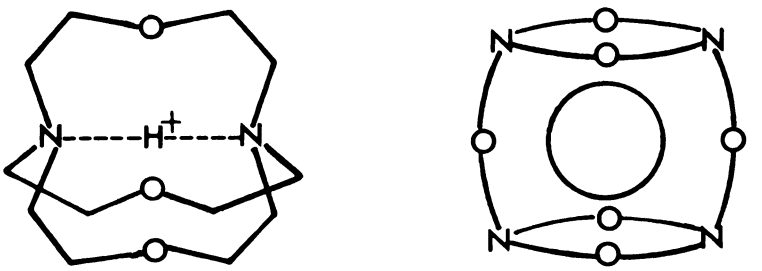

(A) (B)

Figure 5. Structure of (A) "proton" cryptate and (B) "silver" cryptate.

The selectivity factor Ba^{2+}/K^{+} was usually found to be equal or superior to that of nonactin, which was found to be 1/80 by Morf and Simon (95). A complete review paper on all macrocyclic ligands synthesized has been recently published (96).

The kinetics of the complexation were first studied by Lehn (97) by temperature dependent proton NMR on K^{+}-C222 and Na^{+}-C222 cryptates in D_2O solutions. Non-proton NMR has also been found very useful for kinetic studies of the formation of cryptates. Dye and Ceraso (98) studied the exchange rates of sodium cryptate in ethylenediamine and found a free energy of activation value similar to that found by Lehn in aqueous solutions (97). Lehn and Kintzinger (99) measured the ^{23}Na quadrupolar coupling constants of sodium cryptates where the coordination shell is well defined ("frozen" coordination shell). They also obtained rotational correlation times from ^{13}C relaxation time measurements of the methylene carbons of sodium cryptates.

One of the remarkable properties of cryptands is that they can dissolve alkali metals in solvents in which the latter are normally insoluble or only slightly soluble (100). Dye and coworkers (101,102) first found optical evidence for the existence of alkali metal anions (Na^-,K^-) in amine and ether solutions of cryptate salts that they prepared by dissolving sodium or potassium metal with the aid of a crown or a cryptand. They also isolated a Na^- salt (Na^+-C222-Na^-) (103) and determined its crystal structure (194). Recently they published the ^{23}Na NMR spectrum of the sodium anion (105). The ^{23}Na chemical shift of the Na^- resonance was found at 63.2 ppm upfield from saturated aqueous NaCl.

Cryptands with their complexing abilities and potential selectivity are becoming more and more important for many applications in such areas as anion activation, selective cation carriers and formation of alkali metal anions. However, thermodynamic and kinetic data in nonaqueous media are practically nonexistent at the present time. Medium and anion effects must be investigated in order to understand and control the process of complexation of alkali metal cations by cryptand molecules in aqueous and nonaqueous media. Alkali metal nuclear magnetic resonance and vibrational spectroscopy can be very useful techniques to obtain some thermodynamic and kinetic information and such an investigation is presented in Chapter IV, Part II, of this dissertation.

CHAPTER II

EXPERIMENTAL PART

A. SALTS

Lithium perchlorate and lithium chloride (Fisher) were dried at 190°C for several days. The water content was found to be 0.2% and 0.6% by weight, respectively. Lithium iodide (K & K Laboratories) was purified by recrystallization from acetone and dried under vacuum over P_2O_5 for two days at room temperature, and for one day at 56.3°C. The purified salt contained 0.1% by weight of water. Lithium bromide (reagent grade, Matheson Coleman and Bell) was dried at 190°C for three days and contained 0.3% by weight of water. Lithium tetraphenylborate was prepared from $NaBPh_4$ (J. T. Baker) by the methathesis reaction with LiCl (1), then dried over P_2O_5 under vacuum for 12 hours at room temperature, followed by 24 hours at 80°C. The purified salt contained 0.1% by weight of water. After drying, all the lithium salts were stored in a drybox under dry nitrogen atmosphere. Reagent grade iodine (Baker) was used as received. Triiodide solutions were prepared by the addition of equimolar amounts of iodine to a lithium iodide solution in a given solvent. The preparation of ^6Li salts is described in Reference (12).

B. LIGANDS

Trimethylenetetrazole and hexamethylenetetrazole were prepared and purified by previously described techniques

(59). Pentamethylenetetrazole, glutarimide, 3-methyl-3-ethylglutarimide and 3,3-dimethylglutarimide were obtained from Aldrich and were dried under vacuum.

Cryptand 211 (C211) and cryptand 221 (C221) were obtained from E. M. Laboratories, Inc. and were used as received. Lithium-7 NMR measurements indicate that their purity is $\geq$ 98%. Cryptand 222 (C222) was prepared by a modification (81) of the method of Dietrich, et al. (77).

C. SOLVENTS

Nitromethane (spectroscopic grade, Aldrich) was fractionally distilled and dried over freshly activated 5A Linde molecular sieves for 24 hours. Water content was found to be <50 ppm. Dimethylsulfoxide (Baker, reagent grade), was dried over molecular sieves for 2 days; water content, <25 ppm. Acetone (Fisher) was distilled over Drierite and further dried over molecular sieves. Methanol (Analyzed Reagent Grade, Matheson, Coleman and Bell) was first fractionally distilled from calcium hydride and then from magnesium turnings in a nitrogen atmosphere; water content, <40 ppm. Dimethylformamide (Fisher) was vacuum distilled over P_2O_5; water content, <100 ppm. Propylene carbonate (Aldrich), was dried over activated molecular sieves for 2 days. Tetrahydrofuran (Baker, analyzed reagent) was fractionally distilled from calcium hydride

in nitrogen atmosphere; water content, <100 ppm. Acetonitrile (Baker, analyzed reagent) was refluxed over calcium hydride and then fractionally distilled over granulated barium oxide, water content, <100 ppm. Pyridine was refluxed over granulated barium oxide and then fractionally distilled in nitrogen atmosphere. Tetramethylguanidine was refluxed over granulated barium oxide and then fractionally distilled; water content <85 ppm. Acetic acid (Baker) and Formamide (Fisher) were purified by six fractional freezings.

The molecular sieves used were activated by heating them at 500°C under dry argon for 12 hours. Analyses for water in salts and solvents, where possible, were carried out with an automatic Karl Fischer titrator Aquatest II from Photovolt Corp. Important solvent properties and solvent abbreviations are listed in Table II.

D. SAMPLE PREPARATION

Since lithium salts and solvents are very hygroscopic, the water content of each solution was carefully maintained at the lowest possible level so that its total concentration remained less than 1% of the salt concentration. Most of the solutions were prepared in a dry-box under nitrogen. Dilute solutions of salt were prepared by appropriate dilutions of a stock solution. Ligands were weighed out in the desired amount into an appropriate

Table II. Key Solvent Properties and Correction for Magnetic Susceptibility on DA-60.

Solvents	Volumetric Susceptibility-$\times 10^6$	Dielectric Constant	Gutmann's Donor Number	Correction on DA-60 (ppm)
Acetic Acid	0.551	6.18	----	-0.354
Acetone	0.460	20.7	17.0	-0.545
Acetonitrile	0.534	37.5	14.1	-0.390
Chloroform	0.740	4.73	----	0.042
Dimethylformamide (DMF)	0.573	36.71	26.6	-0.308
Dimethylsulfoxide (DMSO)	0.605	46.68	29.8	-0.241
Formamide	0.551	109.5	24.7*	-0.354
Methanol	0.515	32.7	25.7*	-0.429
Nitromethane	0.391	35.9	2.7	-0.689
Propylene Carbonate (PC)	0.634	65.0	15.1	-0.180
Pyridine	0.612	12.40	33.1	-0.226
Tetrahydrofuran (THF)	0.613	7.58	20.0	-0.224
Tetramethylguanidine (TMG)	0.590	11.0	----	-0.272
Water	0.720	78.54	33.0*	0.000

*Predicted (39).

volumetric flask (1 ml, 2 ml or 5 ml) and then introduced into a dry-box for subsequent manipulation.

E. INSTRUMENTAL MEASUREMENTS

1. Lithium-7 NMR

Lithium-7 nuclear magnetic resonance measurements were obtained using a Varian Associates DA-60 spectrometer operating at a field of 1.4092T and a frequency of 23.287 MHz. The spectrometer was frequency locked to an appropriate reference solution (4.0M $LiClO_4$ in water, 3.5M $LiClO_4$ in nitromethane, 3.5M $LiClO_4$ in acetone or 5.0M $LiClO_4$ in methanol) contained in a 1 mm melting point capillary and centered in the 5 mm NMR tube by Delrin spacers. All the chemical shifts reported in this thesis are with respect to 4.0M $LiClO_4$ aqueous solution or aqueous $LiClO_4$ at infinite dilution, as specified. A positive shift from the reference is upfield.

The chemical shifts reported are corrected for differences in bulk diamagnetic susceptibility between sample and reference according to the following equation:

$$\delta_{corr} = \delta_{obs} + \frac{2\pi}{3}(X_v^{ref} - X_v^{sample}) \qquad (1)$$

where X_v^{ref} and X_v^{sample} are the volume susceptibility of the reference and sample solutions respectively and δ_{obs} and δ_{corr} are the observed and the corrected chemical

shifts. Values of δ_{corr} were calculated on the basis of published magnetic susceptibilities of various solvents (106). Several of these values were confirmed by using the method of Live and Chan (107) which involves the measurement of the chemical shift of lithium salt solutions at two different field strengths. The magnitude of the correction for various solvents is shown in Table II. When the contribution of the salt to the magnetic susceptibility of the solution could not be assumed negligible, volume susceptibility of each solution was measured using a Guoy balance. Temperatures were measured with a calibrated thermocouple. Pressurized NMR tubes (30 to 60 psi of N_2) were used when it was necessary to record a spectrum above the boiling point of the solution.

2. Chlorine-35 NMR

Chlorine-35 spectra were obtained with the DA-60 spectrometer operating at a field of 1.0378T and a frequency of 4.33 MHz. Modulation frequencies in the ranges 20-30 Hz and 800-1000 Hz were used, depending on the linewidth to be observed. Care was taken to avoid modulation broadening; the modulation amplitude was progressively reduced until the width of the resonance being observed showed no further narrowing. The radio frequency power and sweep rate were also optimized. All experiments were done at room temperature (25°C). Cylindrical nonspinning sample tubes of about 15 mm diameter were used. Spectra were

calibrated using the high frequency sidebands in the case of relatively narrow lines. Line widths were determined with an estimated accuracy of ±10% as an average of two to four measurements.

Viscosities of lithium perchlorate solutions were measured with an Ostwald viscometer at 25°C in a constant temperature bath.

3. Infrared Spectra

Far infrared measurements (600-50 cm^{-1}) were performed on a Digilab FTS-16 Fourier transform spectrometer. The theory and operation of this instrument have been described by P. Handy (49). Most of the spectra were obtained at a nominal resolution of either 2 or 4 cm^{-1}. A standard demountable Barnes liquid cell with polyethylene windows and a 0.1 mm path length was used.

4. Laser Raman Spectra

Raman spectra were obtained on the Spex Ramalog 4 Laser-Raman system equipped with the Spectra-Physics model 164 argon-ion laser. The 5145 Å line was employed for excitation and data were obtained in the pulse counting mode with a nominal resolution of 2-4 cm^{-1}. Samples were injected into 1.6-1.8 × 90 mm melting point capillary tubes and sealed.

5. Data Handling

Extensive use of the CDC-6500 computer was made to evaluate data. Program KINFIT (108) was employed to determine complexation constants (Appendix II), exchange rates and activation energies (Appendix III).

CHAPTER III

SPECTROSCOPIC STUDIES OF IONIC INTERACTIONS BY LITHIUM-7 NMR, CHLORINE-35 NMR AND RAMAN SPECTROSCOPY

A. INTRODUCTION

Previous studies in this laboratory (35) and elsewhere (28, 40, 109) have shown that sodium-23 NMR offers a very sensitive probe of the environment of sodium ions in various solvents and solvent mixtures. The purpose of this study is to extend such investigations to salts of other alkali metal ions in order to determine the influence of the cation on the ionic equilibria and ionic species present in various nonaqueous solvents.

The exchange of ions between different environments is usually rapid with respect to the NMR time scale, resulting in only one resonance signal at an average frequency determined by the magnetic shielding and lifetime of the nucleus in each of the sites. Alteration of parameters such as concentration, counter ions and solvent produces changes in the relative proportion and type of environment which may be reflected by a change in chemical shift and/or line shape and/or line width of the observed resonance.

The properties of ^{7}Li nucleus are quite favorable for NMR studies. The resonance lines of Li^{+} ion in solutions are exceptionally narrow and chemical shifts can be measured with considerable accuracy (41).

B. RESULTS AND DISCUSSION

Variation of the ^{7}Li chemical shifts with concentration for various salts in various solvents is shown in Appendix

I. In dimethylformamide (DMF) the ^7Li chemical shifts for lithium perchlorate, chloride, bromide and iodide are essentially independent of the counter ion and of the concentration (Figure 6). Somewhat similar behavior is found in propylene carbonate, methanol, and dimethylsulfoxide (DMSO) (Figures 6-7). In tetrahydrofuran (THF), there is little concentration dependence but a significant difference in the chemical shifts of various lithium salts (Figure 8). Acetonitrile (CH_3CN) and nitromethane (CH_3NO_2) solutions show considerable dependence of the ^7Li chemical shift on the concentration and on the counter ion (Figure 9).

Since the limit of detection of ^7Li resonance with our instrument is $\sim$0.01M, it was difficult to establish the limiting chemical shifts of Li^+ ions in such solvents as acetonitrile, THF, nitromethane and acetone where ion pair formation was especially evident. It has been shown previously by electrical conductance measurements that in general, the triiodide salts behave as strong electrolytes in nonaqueous solutions with high and medium dielectric constants (110). It was found that the chemical shifts of lithium triiodide were essentially independent of concentration in all solvents tried and, therefore, the values of the chemical shifts in 0.02 M LiI_3 solutions are reasonably close to the limiting chemical shifts of the Li^+ ion in the same solvents (Table III). It should be noted that in cases where extrapolations of chemical

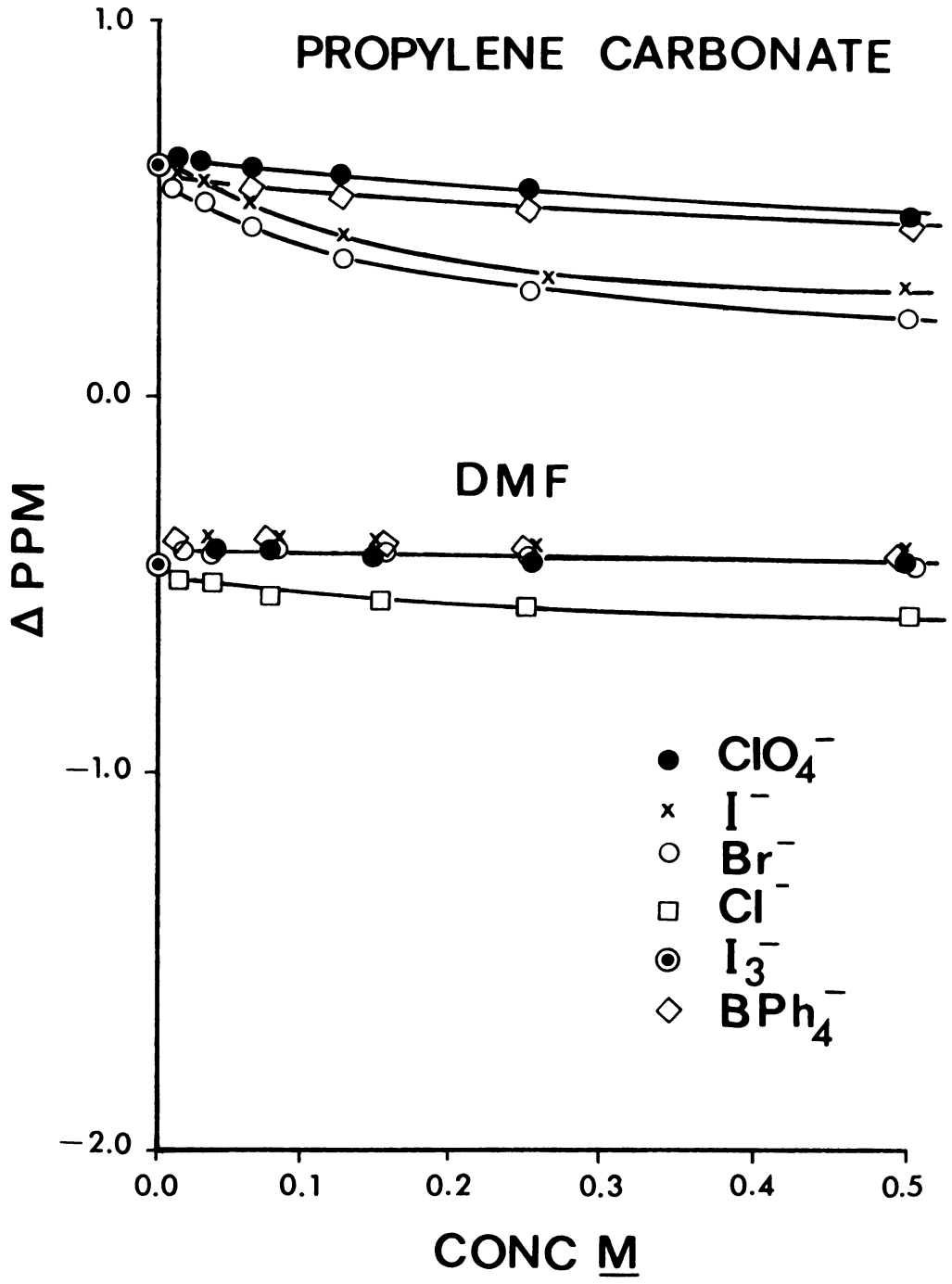

Figure 6. ^{7}Li chemical shifts of lithium salts in propylene carbonate and dimethylformamide.

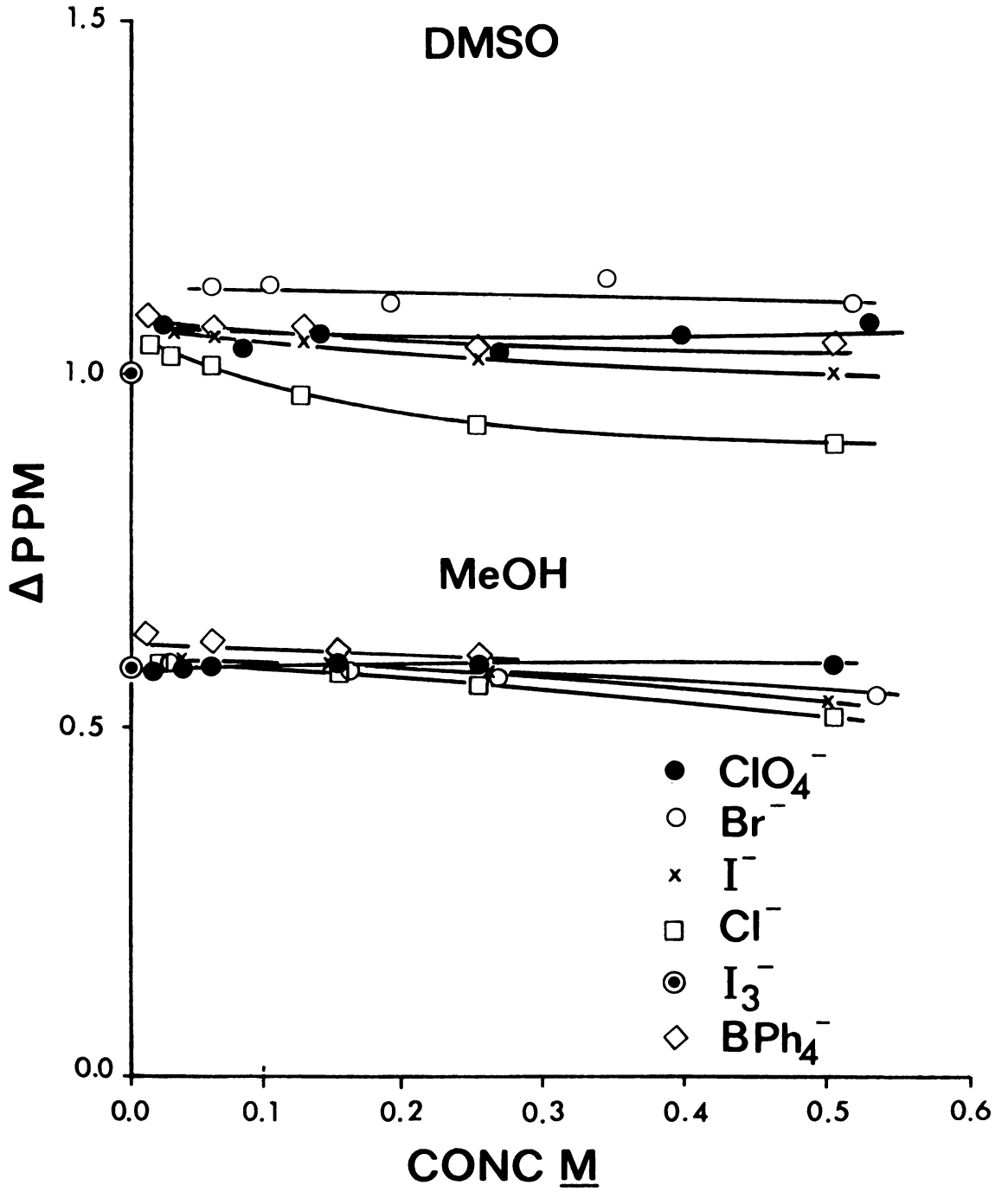

Figure 7. ^{7}Li chemical shifts of lithium salts in dimethylsulfoxide and methanol.

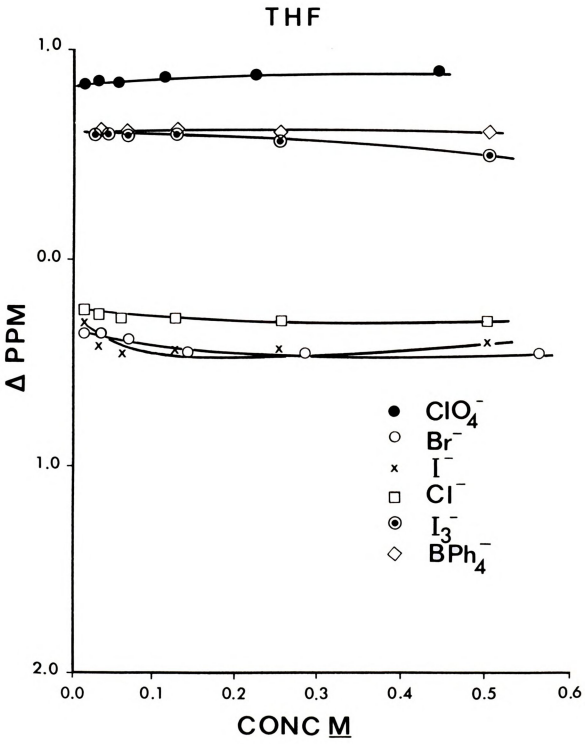

Figure 8. ^{7}Li chemical shifts of lithium salts in tetrahydrofuran.

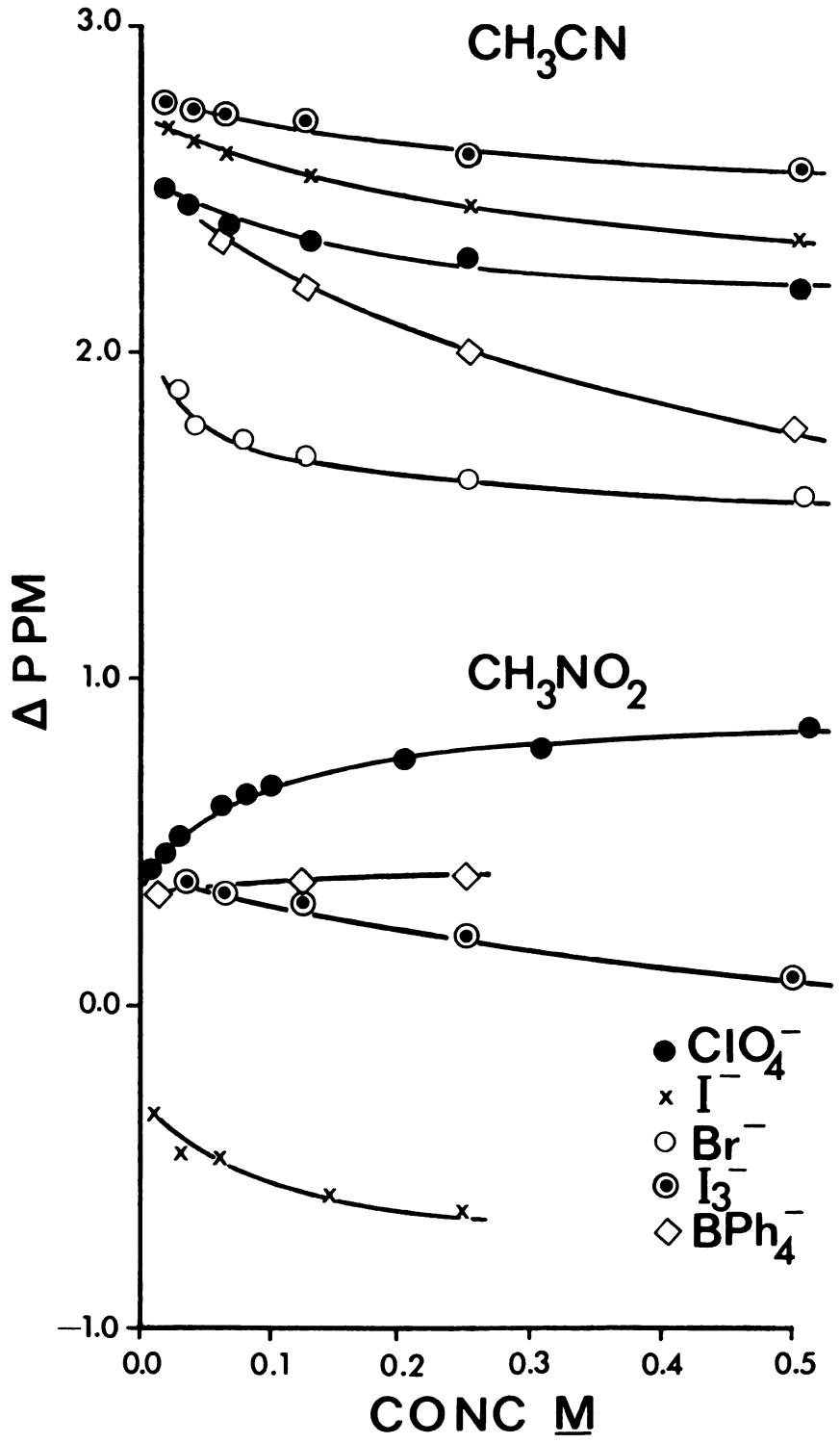

Figure 9. ^{7}Li Chemical shifts of lithium salts in acetonitrile and nitromethane.

Table III. Limiting Chemical shifts of ^{7}Li (0.02M LiI_3) in various solvents.

Solvent	δ(ppm)[a]	Donor Number[b]	Dielectric Constant (25°C)
Acetonitrile	+2.80	14.1	37.5
Dimethylsulfoxide	+1.01	29.8	46.68
Propylene Carbonate	+0.61	15.1	65.0
Tetrahydrofuran	+0.60	20.0	7.58
Methanol	+0.54	25.7[c]	32.7
Nitromethane	+0.36	2.7	35.87
Acetic Acid	+0.03	----	6.2
Dimethylformamide	-0.45	30.9	36.71
Tetramethylguanidine	-0.63	----	11
Acetone	-1.34	17.0	20.7
Pyridine	-2.54	33.1	12.4

[a] Vs 4.0M aqueous $LiClO_4$ as external standard. Corrected for bulk susceptibility.

[b] Ref. (38).

[c] Ref. (35).

shifts to infinite dilution are possible, the value obtained for LiI_3 agrees well with the extrapolated value (for example, in dimethylformamide, methanol and propylene carbonate solutions).

The chemical shift values obtained in this investigation agree reasonably well with those reported by Maciel et al. (44) and by Akitt and Downs (41). Our values, however, seem to be uniformly displaced by $\sim$0.2 ppm towards higher field. This difference may be due to the fact that we have included corrections for the bulk susceptibility of the solvents.

It should be noted that in most solvents with low or intermediate solvating ability, the ^7Li chemical shifts are strongly influenced by the presence of even small amounts of water. It has been shown by Akitt and Downs (41) that the addition of small amounts of water to lithium perchlorate solutions in pyridine results in a sharp upfield shift of the ^7Li resonance. It was found that this effect is even more drastic in non-solvating solvents such as nitromethane. Since most organic solvents cannot be obtained completely anhydrous, it is obvious that in such cases meaningful chemical shifts for Li^+ ion can only be obtained if the concentration of water is much smaller than the concentration of the salt.

It has been previously observed (35, 111) that the contact ion pair equilibrium strongly depends on the donor ability of the solvent molecule as well as on the bulk

dielectric constant of the medium. Although nitromethane has a high dielectric constant of 36, its donor ability is very low and on Gutmann's scale (38), its donor number is 2.7. We see from Figure 9 that the chemical shifts of lithium perchlorate and lithium iodide are concentration dependent and, therefore, that there is contact ion pair formation. There is also some evidence for contact ion pair formation in lithium iodide and bromide solutions in propylene carbonate (Figure 6), (dielectric constant 65, donor number 15.1). These results are in agreement with the data obtained with ^{23}Na NMR in propylene carbonate solutions where the chemical shifts of sodium bromide and of sodium thiocyanate are strongly concentration-dependent (17). On the other hand, in dimethylformamide, with a high dielectric constant of 36.7 and a donor number of 30.9, there is very little influence on the chemical shift by the counter ion or by concentration (Figure 6). In fact, the chemical shifts for the perchlorate, bromide and iodide are essentially superimposable and only the chloride shows some evidence of contact ion pair formation.

Tetrahydrofuran is an interesting solvent in that it has a low dielectric constant of 7.58 but a respectable donor number of 20.0. The similarity of the chemical shifts for the chloride, bromide and iodide (Figure 8), and the fact that they are downfield from the perchlorate, may indicate contact ion pair formation. The low dielectric constant would preclude any ion pair dissociation in the concentration

range used (0.01-0.6M). In fact, conductance measurements reported in a previous paper (35) showed that sodium-anion ion pairs do not dissociate in the same concentration range.

In the case of acetic acid solutions (Figure 10) we see very little concentration or counter ion dependence of the ^{7}Li chemical shift. In fact, the greatest difference we observe is ~0.2 ppm between 0.5M solutions of the perchlorate and the triiodide. Acetic acid, however, is a solvent of low dielectric constant (6.3 at 25°C) and it is natural to expect that there will be a considerable amount of ionic association in this medium. It seems reasonable to assume that in this case we have largely solvent-separated ion pairs and that a very slight concentration dependence indicates an equilibrium between solvent-separated ion pairs and a small amount of contact ion pairs. At the limiting concentration of 0.01M essentially only solvent-separated ion pairs exist in solution. This assumption is strongly supported by a previously reported observation from this laboratory that in acetic acid solution the frequency of the lithium ion vibration in a solvent cage is independent of the nature of the counter ion and comes at 390 cm^{-1} for ^{7}Li salts and at 407 cm^{-1} for ^{6}Li salts (14). On the other hand it has been shown that the frequency of the solvation band is anion-dependent when the anion penetrates the inner solvation shell to form a contact ion pair (7,17,69).

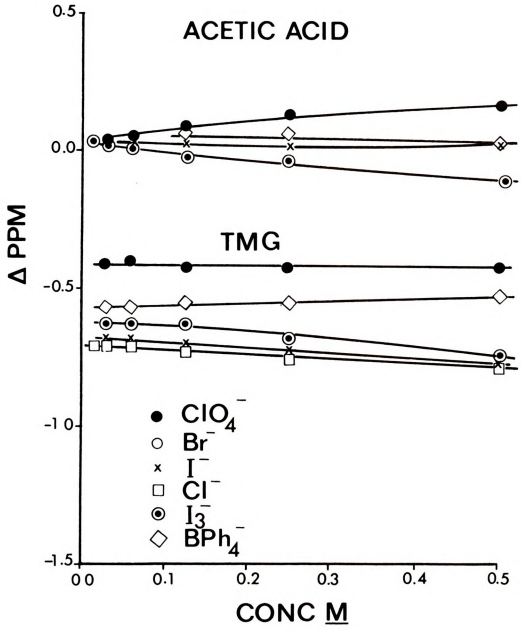

Figure 10. ^{7}Li chemical shift of lithium salts in acetic acid and tetramethylguanidine.

We mentioned above that we attribute the concentration dependence of the ^{7}Li chemical shifts to the formation of contact ion pairs, i.e., to cases where the anion directly replaces a solvent molecule or molecules in the inner solvation shell of the cation. It seems reasonable to assume that gross variations in the chemical shift of an alkali metal ion is a direct influence of the change in its immediate chemical environment, i.e., it reflects the influence of its nearest neighbors. It has been shown, for example, that NMR techniques for the determination of solvation numbers of ions invariably yield numbers indicative of the inner solvation shell. Thus the hydration number of magnesium (II) ion was found to be six by the NMR measurements (112) while electrical conductance technique, which also reflects the contribution of the outer solvation (113) shell, yields a solvation number of 14-15.

The results of the ^{35}Cl NMR study are shown in Table IV. In general, in dilute solutions the width at half height of the ^{35}Cl resonance was 10-20 Hz as compared with 45 or 65 Hz reported previously for aqueous solutions. It is seen that there is a considerable broadening of the ^{35}Cl resonance with increasing concentration of the salt in nitromethane and to some extent in tetrahydrofuran and tetramethylguanidine. On the other hand, very little concentration dependence is evident in acetone, methanol or acetonitrile solutions.

It seems that the concentration-dependent broadening

Table IV. Line broadening of ^{35}Cl resonance in $LiClO_4$ solutions.

Solvent	Conc (M)	$W_{1/2}$[a] (obs,Hz)	η(cp)sample / η(cp)solvent	$W_{1/2}$[a] (corr,Hz)
Acetone	0.26	11	1.12	10
	0.52	16	1.21	13
	1.00	27	2.07	13
	1.49	38	2.63	14
	2.03	55	3.80	14
	2.52	84	6.22	13
	3.02	142	10.82	13
	3.50	257	19.29	13
	4.00	485	32.16	14
Methanol	0.49	19	1.30	15
	1.00	19	1.37	14
	1.99	26	1.90	14
	4.00	43	3.76	11
	5.98	121	9.14	13
Nitromethane	0.26	85	1.04	82
	0.51	120	1.16	103
	1.01	178	1.40	127
	1.50	220	1.67	132
	2.00	260	1.97	132
	2.50	304	2.46	124
	3.02	325	2.66	122
Tetrahydrofuran	0.26	53	1.19	44
	0.49	63	1.39	45
	1.44	202	3.14	64
	2.01	349	5.19	67
Tetramethylguanidine	1.00	280	5.52	51

Table IV - continued

Solvent	Conc (M)	$W_{1/2}$[a] (obs,Hz)	η(cp) sample / η(cp) solvent	$W_{1/2}$[a] (corr,Hz)
Acetonitrile	0.26	15	1.10	14
	0.50	27	1.26	21
	1.00	36	1.67	22

[a]Width at half height.

of the ^{35}Cl resonance is indicative of contact ion pair formation for the reasons given below.

In theory, spin-lattice relaxation mechanisms may be divided into five categories (114): dipole-dipole relaxation, chemical shift anisotropy, scalar coupling, spin-rotation relaxation, and quadrupole relaxation. Since the observed relaxation time is assumed to be in the motionally narrowed limit so that T_1 equals T_2, the observed results may be expressed as:

$$\frac{1}{T_1} = R_{1\ exp} = R_{1\ dip\text{-}dip} + R_{1\ scalar} + R_{1\ \substack{chem\\shift\\anis}}$$

$$+ R_{1\ spin\ rot} + R_{1\ quad} \qquad (2)$$

In general, the relaxation mechanisms have a Hamiltonian operator

$$H_c = -hI.T_c.0 \qquad (3)$$

where I is the spin of interest, 0 is a physical quantity which interacts with I to provide the relaxation mechanism, and T_c is the coupling interaction tensor. For the case of the dipole-dipole relaxation mechanism we have

$$H_c = hI.T.S \qquad (4)$$

where S is the nuclear spin of the species coupled to the spin of the nucleus of interest. Clearly, this relaxation mechanism is negligible when compared to smallest observed R_1 for ^{35}Cl in the $^{35}ClO_4^-$ anion. Since the interaction falls off as r^{-3}, where r is the distance between spins, dipole-dipole interactions between ^{35}Cl and nuclei other than nearest neighbors need not be considered, at least to a first approximation.

For chemical shift anisotropy to be a significant relaxation mechanism, the chemical shift of the species must vary radically with orientation in the magnetic field. The ClO_4^- anion cannot satisfy this criterion, since even a fairly large deviation from T_d symmetry does not seem to affect chemical shift significantly.

Scalar coupling of the first kind is due to the effects of chemical exchange of the species of interest, or of nuclei directly coupled to it. This is of no relevance to ^{35}Cl resonance of the ClO_4^- anion, since the nonexchanging oxygens shield the chlorine effectively from chemical exchange effects. In contrast, scalar coupling of the second kind would be due to magnetic field fluctuations at the chlorine nucleus due to motion of the ^{17}O nuclear spins, which should be negligible compared to the observed R_1 as a consequence of the extreme magnetic dilution of ^{17}O.

In the isotropic molecular reorientation limit, the contribution from the spin rotation mechanism may be expressed as

$$R_{1\ \substack{spin\\rot}} = \left(\frac{2\pi IkT}{h^2}\right) C_{eff}^{\ 2} \tau_\theta \qquad (5)$$

where I is moment of inertia of the ClO_4^- anion, C_{eff} is the spin rotation coupling constant and τ_θ is the angular correlation time. A calculation using the largest reasonable estimates of τ_θ and C_{eff} shows that $R_{1\ spin\ rot}$ is several orders of magnitude smaller than the smallest observed $R_{1\ exp}$.

The term involving quadrupole relaxation may be expressed as

$$R_1 = R_2 = \frac{3}{40} \frac{2I+3}{I^2(2I-1)} \left(1 + \frac{\eta^2}{3}\right) \left(\frac{e^2Qq}{h}\right)^2 \tau_c \qquad (6)$$

where I is the nuclear spin of the observed species, η is the assymmetry parameter, e^2Qq/h is the quadrupole coupling constant, and τ_c is the translational correlation time. For $^{35}ClO_4^-$, the assymmetry parameter is zero, or at most very small for small distortions from T_d symmetry, and the terms involving the nuclear spin are of course constant. Therefore concentration dependence of $R_{1\ quad}$ must depend on the influence of concentration on either the correlation time, τ_c, or the quadrupole coupling constant, or both. For pure T_d symmetry, e^2Qq/h is zero, since this term may also be expressed as $(eQ/h)(\partial^2V/\partial z^2)$ (115), and the electric field gradient at the chlorine nucleus is obviously zero for pure tetrahedral symmetry. Therefore, for the quadrupole relaxation mechanism to make any contribution to

R_1, some distortion from T_d symmetry must be involved. Changes in this distortion with concentration and, of course, any change in $R_{1\ quad}$ would be due to an ion pair phenomenon rather than classical solvation or bulk viscosity effects. Also it should be noted that changes in the electric field gradient at the chlorine nucleus affect the $R_{1\ quad}$ as the square of the perturbation, while τ_c is influential only to the first power. Several authors have assumed that this effect on the translational correlation time might be minimized by using a correction term linear in bulk viscosity, but recently (116,117) this correction term has been questioned on the basis that bulk viscosity does not accurately reflect changes in τ_c, especially for relatively high concentrations ($>10^{-2}$ M). Despite this, the correction is still useful in predicting the sign and order of magnitude of the change in $R_{1\ quad}$ due to the concentration effects on τ_c.

In conclusion, it seems that the ^{35}Cl NMR data support our assumption that the concentration-dependent ^{7}Li chemical shifts are indicative of the contact ion pair formation. This is particularly evident in nitromethane as shown in Figure 11. It is, of course, possible that the second nearest neighbors (solvent shared ion pairs) may slightly influence the chemical shift of the alkali nucleus, however, the predominant effect must be due to the nearest neighbors. Similar results were recently obtained by Stengle and coworkers (118) who have studied sodium, lithium and

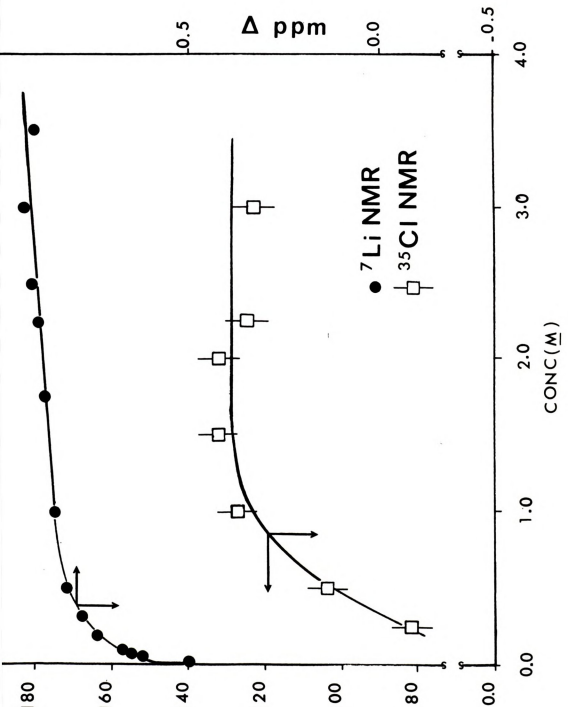

Figure 11. ^{7}Li chemical shift and ^{35}Cl NMR resonance line width of $LiClO_4$ in nitromethane as a function of lithium concentration.

particularly magnesium perchlorates in nonaqueous solvents by ^{35}Cl NMR.

An interesting difference was observed in the relation between the ^{23}Na and ^{7}Li chemical shifts in different solvents and the Gutmann donor numbers (38). It was pointed out in previous publications that a plot of the limiting ^{23}Na chemical shifts vs donor numbers yields a respectable straight line. It is interesting to note that no such correlation is observable with the ^{7}Li chemical shifts in different solvents (Table 3, page 34). For example, the limiting chemical shift of a poor donor, nitromethane, is between the limiting chemical shifts of two excellent donors, dimethylsulfoxide and pyridine.

Several workers (109) have pointed out that in the case of sodium, the paramagnetic screening constant is dominant over the diamagnetic screening constant. For lithium, however, this is not the case; the diamagnetic and paramagnetic terms are of the same order of magnitude, and tend to cancel one another (31). For this reason, effects such as ring currents and neighbor-anisotropy effects become more important for lithium chemical shifts, as pointed out by Maciel et al. (44). For example, in the case of pyridine, the deshielding of the lithium nucleus may be accounted for by the effect of the circulating electrons, if it is assumed that the lithium nucleus is coordinated with the nitrogen in the plane of the ring. Conversely, the upfield shift of the lithium when

coordinated to acetonitrile may be attributed to a strong neighbor-anisotropy effect analogous to the extraordinary shielding of acetylene protons.

Evidence for contact ion pair formation, in the case of lithium perchlorate-acetone system, was also obtained by Popov and coworkers (13) from the behavior of the 935 cm^{-1} Raman band corresponding to the symmetrical stretch of the ClO_4^- ion (ν_1, A_1). They observed that the 935 cm^{-1} perchlorate Raman band splits upon formation of contact ion pairs. Greenberg (39), monitoring the three easily observable perchlorate bands at 935, 460 and 626 cm^{-1} respectively, in $NaClO_4$ solutions, observed a split of the 460 cm^{-1} band in solvents which gave indication of contact ion pairs formation by ^{23}Na NMR; acetonitrile, tetrahydrofuran and pyridine. He observed only a marked broadening of the 935 cm^{-1} band. It is clear then, that the formation of contact ion pairs, which perturbs the T_d symmetry of the ClO_4^- ion, can be observed by Raman spectroscopy.

We monitored the 935 cm^{-1} perchlorate Raman band as a function of $LiClO_4$ concentration in nitromethane, methanol, acetonitrile and tetramethylguanidine (Figures 12 and 13). At high concentration of $LiClO_4$ the 935 cm^{-1} band splits and a new band appears at 938, 940 and 946 cm^{-1} in tetramethylguanidine, methanol and nitromethane, respectively. In acetonitrile the 935 cm^{-1} band becomes unsymmetrical when the $LiClO_4$ concentration reaches 1.0 M.

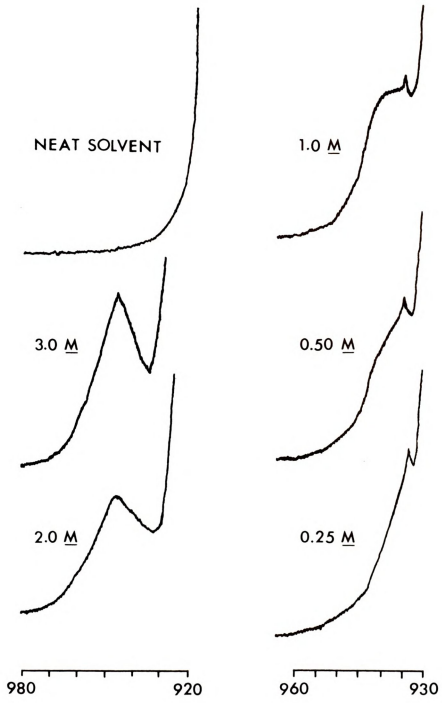

Figure 12. Raman spectra of the ClO_4^- 935 cm^{-1} band as a function of $LiClO_4$ concentration in nitromethane.

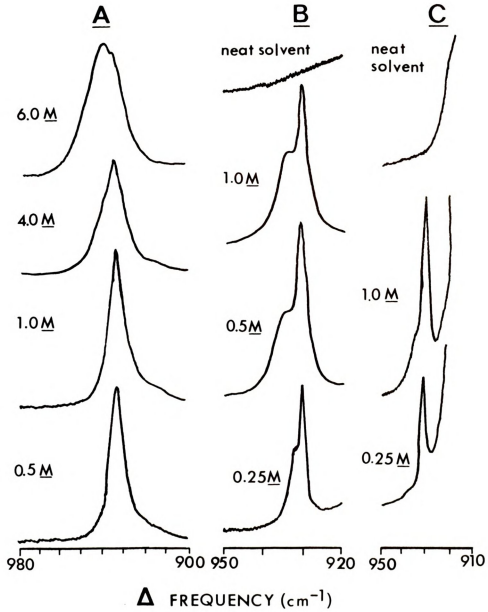

Figure 13. Raman spectra of the ClO_4^- 935 cm^{-1} band as a function of $LiClO_4$ concentration in, (A) methanol, (B) tetramethylguanidine, (C) acetonitrile.

These observations confirm the results obtained by ^{7}Li NMR in nitromethane and tetramethylguanidine where indications of contact ion pairing have been found. In methanol the appearance of the new band occurs only at concentrations higher than 4.0 M, where the deficiency of solvent molecules causes the formation of contact ion pairs.

CHAPTER IV

SPECTROSCOPIC STUDIES OF COMPLEXATION OF ALKALI METAL IONS

I. LITHIUM-7 NMR STUDY OF THE Li^+ COMPLEX WITH CONVULSANT POLYMETHYLENE TETRAZOLES AND GLUTARIMIDES IN NITROMETHANE SOLUTIONS

A. INTRODUCTION

Both 1,5-polymethylenetetrazoles and glutarimides (page 10) are convulsant agents. Small changes in the substituent groups, however, may change drastically the convulsant activity of the compounds. For example, the convulsant activity of polymethylenetetrazoles increases with increasing length of the polymethylene chain. The minimum convulsant dose varies from 1000 mg/kg for trimethylenetetrazole to 30 mg/kg for heptamethylenetetrazole (57). (Tetrazoles with larger methylene chains are insoluble in water.)

While the mechanism of convulsant activity of the above compounds remains unknown, there is a possibility that their interaction with the alkali metal ions of the central nervous system may be an important factor in their physiological activity. Consequently we investigated the interactions of alkali metal ions with convulsant drugs.

Initial studies on alkali ion-tetrazole systems (47) showed that while tetrazoles do form complexes with alkali metal ions, such complexes are very weak and cannot be studied by conventional potentiometric or spectroscopic techniques. On the other hand, alkali metal NMR spectra

are very sensitive probes of the immediate environment of the alkali metal ion and the addition of a tetrazole to a Li^+ or Na^+ salt solution results in a definite shift of the ^7Li or ^{23}Na resonance.

In order to maximize the interaction between the drugs and the lithium ion, measurements were carried out in nitromethane, which is a poorly solvating solvent (although with a high dielectric constant of 35.87) and thus offers a minimum of competition for the complexation reaction with the drug molecules.

B. RESULTS AND DISCUSSION

We assume that in all solutions containing the drug molecule and Li^+ ion, the latter is found in two environments: free solvated lithium ion and the complexed lithium ion. The exchange between the two environments is fast as compared to the NMR time scale, therefore, only the mass-average chemical shift is observed

$$\delta_{obs} = \delta_M X_M + \delta_{ML} X_{ML} \qquad (7)$$

where δ_{obs} is the observed chemical shift, X_M and X_{ML} are respectively the mole fractions of the free and complexed metal ion while δ_M and δ_{ML} are the respective chemical shifts for the two species. Assuming a 1:1 complex, we have the equilibrium

$$M + L \rightleftharpoons ML \tag{8}$$

where L is the ligand. The formation constant of the complex, in concentration units, becomes

$$K = \frac{C_{ML}}{C_M C_L} \tag{9}$$

where C_M and C_{ML} are the equilibrium concentrations of free ligand and of the complex respectively. Equation (7) can be written as:

$$\delta_{obs} = (KC_M^t - KC_L^t - 1) \pm (K^2C_L^{t\,2} + K^2C_M^{t\,2} - 2K^2C_M^tC_L^t + 2KC_L^t + 2KC_M^t + 1)^{\frac{1}{2}}$$

$$\frac{\delta_M - \delta_L}{2KC_M^t} + \delta_{ML} \tag{10}$$

Since δ_M can be easily determined from measurements on solutions of lithium salts without the ligand, and C_M^t and C_L^t, respectively, the total concentration of metal ion and ligand, are known, Eq. (10) contains two unknowns K and δ_{ML}. For a fairly strong complex δ_{ML} can be determined experimentally by the addition of such excess of L that essentially all of the metal is in the complexed form. For a weak complex, however, either the limiting shift value is unobtainable or such large excess of L is needed that the solution loses even a semblance of ideality.

The procedure we use for solving Eq. (10) is to substitute the experimental parameters δ_{obs}, C_M^t, C_L^t and δ_M

and vary K and δ_{ML} until the calculated chemical shifts correspond to the experimental values within the error limits on concentration (0.01 M) and shifts (0.05 ppm). The data were analyzed on a CDC-6500 computer using the Fortran IV program KINFIT (108). A more detailed derivation and the description of the subroutine EQN used are given in Appendix II.

A typical plot of experimental points and of the computer-generated curve for Li^+-3,3-dimethyl glutarimide system is shown in Figure 14. It is seen that a satisfactory agreement is obtained between the calculated and the experimental values. Similar plots were obtained for other systems. The results are given in Table V.

Both glutarimides and polymethylenetetrazoles form complexes with the lithium ion in a non-solvating (or poor donor) solvent such as nitromethane. In aqueous solutions, where alkali cations are much more strongly solvated, the competition between the solvent molecules and the relatively weak ligand, glutarimides or tetrazoles, may be heavily weighted in favor of the solvent and the complexation constant would be much smaller.

As seen from Table V, the formation constants of the lithium-drug complex are dependent on the total concentration of the lithium salt, C_M^t. The inconstancy of the K_f values may be due to (a) activity effects, (b) formation of more than one complex in solution and (c) competing equilibria involving $Li^+ClO_4^-$ ion pairs. Since the

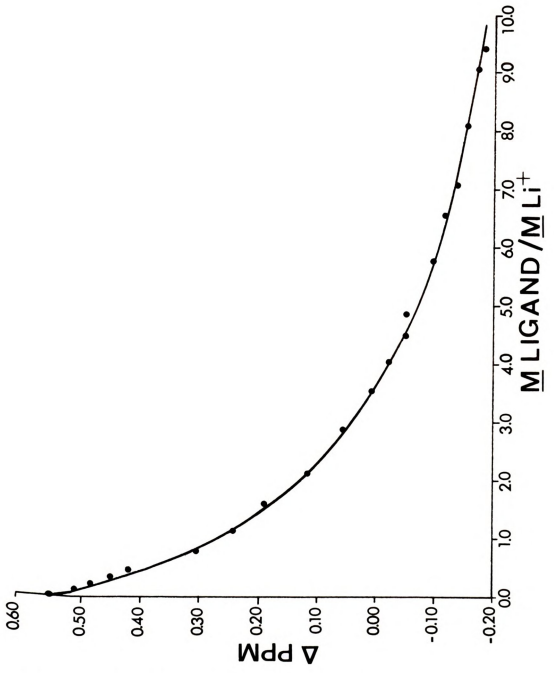

Figure 14. Plot of ^{7}Li chemical shift with reference to 4.0 M aqueous $LiClO_4$ vs mole ratio of 3,3-dimethyl glutarimide to Li^+ at constant $[Li^+]$ = 0.100 M. Solid line is computer-generated curve and dots are the experimental points.

Table V. Formation Constants of Li^+-Tetrazoles and Li^+-Glutarimides Complexes.

Formation Constants of Li^+-Tetrazoles

Ligand	Conc of $LiClO_4$ (M)	Ligand Conc Range (M)	Kf (M^{-1})
Trimethylenetetrazole	0.000	b	6.25±0.10
	0.050	0-2.3	4.97±0.10
	0.104	0-3.0	3.73±0.05
Pentamethylenetetrazole	0.000	b	4.85±0.10
	0.011	0-0.9	4.54±0.10
	0.050	0-2.5	3.19±0.09
	0.100	0-3.2	1.72±0.10
Hexamethylenetetrazole	0.000	b	5.05±0.10
	0.011	0-1.0	4.91±0.07
	0.104	0-1.5	3.85±0.06

Formation Constants of Li^+-Glutarimides

Glutarimide	0.000	b	9.3±0.4
	0.010	0-1.0	9.0±0.4
	0.050	0-1.0	7.6±0.3
	0.099	0-1.4	6.0±0.4
3-Ethyl-3-methyl glutarimide	0.000	b	7.6±0.3
	0.010	0-0.8	7.4±0.3
	0.049	0-0.8	6.8±0.2
	0.100	0-1.0	5.9±0.2
3,3-Dimethyl glutarimide	0.012[a]	0-1.0	6.6±0.3

[a]Complex precipitated out at higher lithium concentrations.
[b]Extrapolated value.

complexation reaction does not involve separation of charges and since the solutions are relatively dilute, the activity effects should be minimal. The formation of 2:1 complex seems to be excluded by the very good agreement between the experimental and calculated chemical shifts, especially at high ligand/Li^+ mole ratios where formation of 2:1 complex should be more apparent. In addition, results from ^7Li NMR in various solvents presented in Chapter I of this thesis, strongly indicate ion pair formation in nitromethane solutions of lithium perchlorate. Consequently, we assume that the competing equilibrium with $Li^+ClO_4^-$ ion pairs is the principal cause for the variation of K_f values with salt concentration.

Plots of K_f vs. lithium ion concentration are essentially linear (Figure 15). Extrapolation to infinite dilution should yield quasi-thermodynamic constants for the complexation reactions.

The lithium complexes of polymethylenetetrazoles appear to be more stable than the corresponding complexes of the sodium ion. For example, the formation constant of the pentamethylenetetrazole-Na^+ complex in nitromethane is 0.76 (48) as compared with 4.85 for lithium.

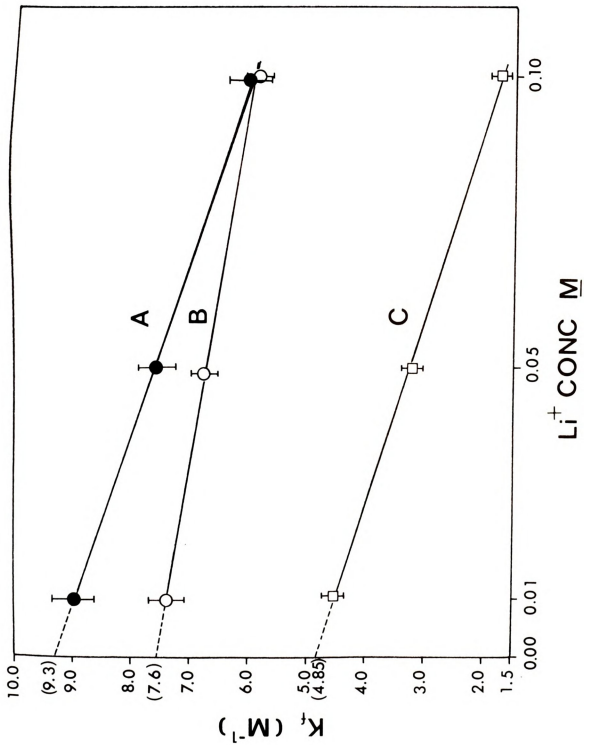

Figure 15. Plot of formation constants vs lithium ion concentration. A - Glutarimide. B - 3-ethyl-3-methyl glutarimide. C - Pentamethylenetetrazole.

II. STUDY OF THE COMPLEXATION OF ALKALI METAL IONS BY CRYPTAND LIGANDS IN VARIOUS SOLVENTS

A. LITHIUM-7 NMR STUDY

1. Lithium-7 Chemical Shift of Lithium 222, 221, 211 Cryptates in Various Solvents

The ^7Li chemical shifts were determined as a function of cryptand/Li^+ mole ratios with the results shown in Table VI. Typical spectra obtained with cryptand C211 are shown in Figure 16.

The stability of a cryptate complex is largely determined by the size of the cryptand cavity and the solvating ability of the solvent. If the rate of exchange of the lithium ion between the two sites, free ion in the bulk solution and the complex, is greater than $2/\pi\Delta\nu$, where $\Delta\nu$ is the difference between the characteristic resonance (in Hz) of each site, only one population-average resonance is observed. This is the case with C222 which has a much larger cavity (2.8 Å) than the bare lithium ion (1.56 Å). Only one ^7Li resonance is observed in nitromethane, dimethylsulfoxide, pyridine, and water solutions.

In dimethylsulfoxide and aqueous solutions, the solvent molecules have a strong solvating ability and compete quite successfully with the ligand. Consequently, only a weak lithium complex is formed and a large excess of

Table VI. ^{7}Li - NMR Study of C222, C221, C211, Lithium Complexes in Various Solvents at Room Temperature.

Cryptand 222

Solvent	Salt	$[Li^+]$ (M)	[Cryptand]/$[Li^+]$	^{7}Li Chemical Shift (ppm)[a]
CH_3NO_2	$LiClO_4$	0.025	0.0	0.35
			0.5	0.75
			1.0	1.02
			2.0	1.03
DMSO	$LiClO_4$	0.025	0.0	0.97
			0.5	0.97
			1.0	0.96
			2.0	0.96
Pyridine	$LiClO_4$	0.025	0.0	-1.52
			0.7	0.30
			1.0	1.04
			2.5	1.61
			∞(b)	1.73
H_2O	LiI	0.010	0.0	0.00
			1.0	0.00_5
			10.0	0.09_5
			20.0	0.11
			∞(b)	0.18

Cryptand 221

CH_3NO_2	$LiClO_4$	0.05	0.0	0.38
			0.5	0.81
			1.0	1.04
			2.0	1.03

Table VI - Continued

Cryptand 221 - Continued

Solvent	Salt	$[Li^+]$ (M)	[Cryptand]/$[Li^+]$	^{7}Li Chemical Shift (ppm)[a]
DMSO	$LiClO_4$	0.05	0.0	0.94
			0.5	0.96
			1.0	0.97
			2.0	0.98
Pyridine	$LiClO_4$	0.05	0.0	-2.16
			0.5	-2.21, 1.87

Cryptand 211

CH_3NO_2	$LiClO_4$	0.15	0.0	0.61
			1.0	0.41
	LiI	0.14	0.0	0.49
			1.0	0.42
	LiI_3	0.14	0.0	0.11
			0.4	0.01 and 0.37
			0.9	0.37
	LiCl	0.13	1.0	0.41
DMSO	$LiClO_4$	0.20	0.0	0.97
			0.8	0.95 and 0.39
			1.0	0.39
	LiI	0.14	0.0	0.95
			1.0	0.39

Table VI - Continued

Cryptand 211 - Continued

Solvent	Salt	$[Li^+]$ (M)	[Cryptand]/$[Li^+]$	^{7}Li Chemical Shift (ppm)[a]
	LiCl	0.11	0.0	0.88
			1.0	0.39
	$LiBPh_4$	0.10	0.0	0.97
			1.0	0.42
THF	LiI_3	0.10	0.0	0.48
			0.5	0.44 and 0.36
			1.0	0.36
PC	$LiClO_4$	0.25	0.0	0.45
			0.5	0.52 and 0.38
			1.0	0.38
$CHCl_3$	LiI_3	0.15	1.0	0.38
H_2O	LiI	0.25	0.0	0.00
			0.5	0.00 and 0.38
DMF	$LiClO_4$	0.25	0.0	-0.50
			0.5	-0.40 and 0.42
Formamide	$LiClO_4$	0.25	0.0	-0.39
			0.5	-0.43 and 0.38

[a] Vs aqueous $LiClO_4$ at infinite dilution (corrected for magnetic susceptibility).

[b] Calculated.

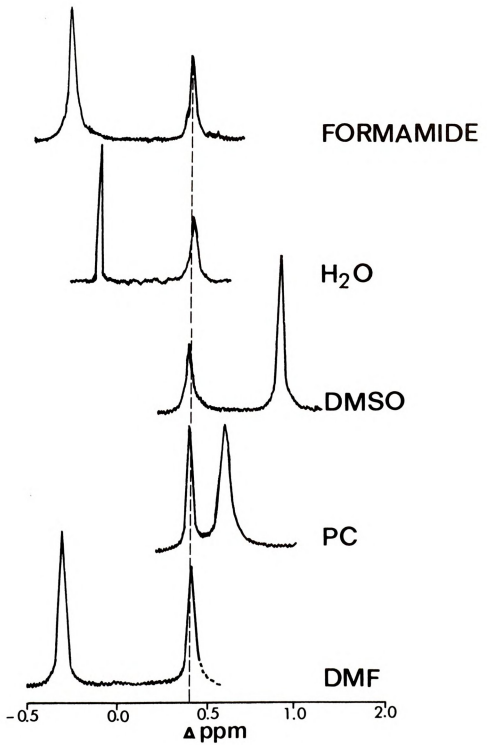

Figure 16. Lithium-7 NMR spectra of lithium-C211 cryptate in various solvents; [C211] = 0.25 M, [Li^+] = 0.50 M. Chemical shift of Li-C211 is at 0.41 ppm vs aqueous $LiClO_4$ solution at infinite dilution.

ligand is necessary to produce a variation of the chemical shift (see Table 6) from the position characteristic of the solvated Li^+ ion in the given solvent. In nitromethane which is a poor solvating solvent, and in pyridine which is a nitrogen donor solvent, the respective complexes are readily formed as evidenced by the chemical shift of the ^7Li resonance upon addition of the ligand.

With cryptand C221 the exchange is slower because of the smaller cavity size of the ligand (2.2 Å). In dimethylsulfoxide C221 forms a weak complex with the Li^+ ion, while in nitromethane the complex is more stable and the limiting chemical shift for Li^+-C221 complex (1.04 ppm) is reached at 1:1 ligand/Li^+ mole ratio. In both cases only one population averaged resonance line is observed because the exchange is fast on the NMR time scale. In pyridine at room temperature the exchange is slow enough and the difference between the chemical shift is large enough (3.89 ppm) so that two ^7Li resonances are obtained, one for the complexed lithium ion at 1.87 ppm and one at -2.02 ppm for the solvated lithium ion *vs* aqueous $LiClO_4$ solution at infinite dilution.

Cryptand 211 has a cavity radius nearly equal to that of the unsolvated lithium ion. It is expected, therefore, that very stable lithium complexes will be formed and that the exchange will be slow. The Li^+-C211 system was investigated in nitromethane, dimethylsulfoxide, tetrahydrofuran, propylene carbonate, chloroform, dimethylformamide,

formamide and water solutions. The data shown in Table 6 indicate that in all solvents the addition of the ligand, in less than stoichiometric amounts, results in two resonances corresponding to the free and the complexed lithium ion. Similar results were found in a ^{23}Na NMR study of sodium-C222 complexes in ethylenediamine (98) and in other solvents (119).

Not surprisingly, the chemical shift of the lithium ion complexed by C211 is essentially independent of the solvent and the counterion used (Figure 16). In all cases it is found at 0.40±0.03 ppm. In the complex, the lithium ion is completely encased by the ligand and since the ^{7}Li chemical shifts are dependent almost exclusively on the nearest neighbors of the lithium ion, they are insensitive to either the solvent molecules surrounding the cryptate or to the counterion in the cases where a low dielectric constant of the solvent (such as THF or chloroform) would lead to ion pair formation.

On the other hand, the limiting chemical shifts of Li^{+}-C222 and especially Li^{+}-C221 complexes are definitely solvent-dependent indicating that the looser structure of the complex permits the solvent molecules to approach sufficiently close to the metal ion to affect its resonance frequency.

Lithium NMR has been shown to be a useful technique for the determination of the formation constants of weak and medium strength complexes (Chapter IV-I). This approach

was used in this work to determine the formation constants of Li^+-C222 complexes in water and pyridine. The technique involves the measurement of ^7Li chemical shifts as a function of ligand/Li^+ mole ratio (Table VII), followed by a computer fit of the data as described in Appendix II. The plot of experimental points of the computer-generated curve for Li^+-C222 in pyridine is shown in Figure 17.

The values obtained were: log K_f = 0.99±0.15 and log K_f = 2.94±0.10 for the formation of Li^+-C222 in water and pyridine, respectively. The previously reported value in methanol (80) is log K_f = 2.65 which reflects its intermediate solvating ability for the lithium ion between that of water and of pyridine. Previous estimates of log K_f values in water were ∿0 and <2 (90,120).

It should be noted that the above values are the concentration constants. However, since the complexation reaction

$$Li^+ + C222 \rightleftarrows Li^+\text{-}C222 \qquad (11)$$

does not involve separation of charges, these values should represent reasonable approximations of the thermodynamic constants.

Table VII. ^{7}Li Chemical Shifts as a Function of Ligand/Li^{+} Mole Ratio for the Determination of the Formation Constants of Li^{+}-C222 Complexes in Water and Pyridine.

Water $[Li^{+}]$ = 0.0102 M		Pyridine $[Li^{+}]$ = 0.0253 M	
$(222)/(Li^{+})$	δ (ppm)[a]	$(222)/(Li^{+})$	δ (ppm)[a]
0.000	0.090	0.000	-1.864
0.501	0.093	0.084	-1.443
0.752	0.096	0.294	-0.803
0.994	0.095	0.315	-0.732
1.447	0.099	0.672	0.528
2.470	0.122	0.724	0.616
4.931	0.142	0.808	0.839
6.614	0.163	0.945	1.147
8.652	0.185	1.071	1.355
9.774	0.185	1.302	1.580
14.793	0.193	1.449	1.679
19.685	0.200	1.732	1.795
		2.079	1.941
		2.614	1.932

[a]Lithium 7 Chemical Shift vs 4.0 M $LiClO_4$ in water.

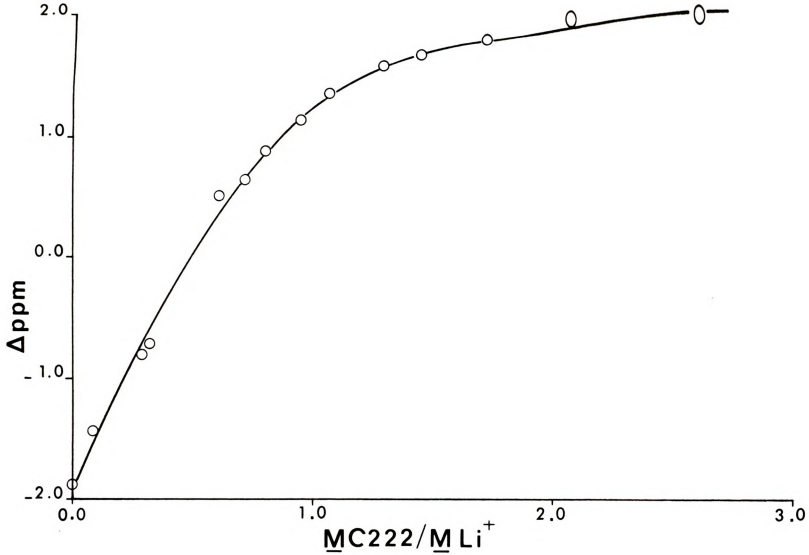

Figure 17. Plot of ^{7}Li chemical shift with reference to 4.0 M aqueous $LiClO_4$ vs mole ratio of cryptand 222 to Li^+ in pyridine at constant $[Li^+]$ = 0.25 M. Solid line is computer-generated curve and dots are experimental points.

2. Lithium NMR Study of the Lithium Ion-Lithium Cryptate Exchange in Various Solvents

The drastic effect of the solvent on the complexation reaction has been illustrated (Chapter IV-II-A-1) by the difference in the formation constants of the Li^+-C222 complex in water and in pyridine. Thus, the strong solvating ability of water drastically depresses the value of the Li^+-C222 formation constant. We have seen also that the lithium ion forms stable complexes with the cryptand 211, and the exchange between the free and the bound lithium ion is slow on the NMR time scale. Thus, solutions containing lithium in excess can be examined by measuring the ^7Li resonances. The exchange kinetics can be deduced from changes in line shapes as a function of temperature.

The complexation process between a ligand and a cation M^+ in a solvent S can be represented by the following general equation,

$$L + M^+_{solv} \underset{k_b}{\overset{k_f}{\rightleftharpoons}} LM^+ + solvent \qquad (12)$$

which assumes a first order process for the backward reaction, e.g. in our case, the dissociation reaction or the release of the lithium ion from the cryptate cavity. Such a mechanism was found to be predominant for the complexation of sodium ions by dicyclohexyl-18-crown-6 (121). The general case of exchange between two sites A and B with

different relaxation times is described by the following modified Bloch equations (98,122)

$$G = u + iv \tag{13}$$

$$v = -\gamma H_1 M_0 \left(\frac{SU + TV}{S^2 + T^2} \right) \tag{14}$$

$$u = -\gamma H_1 M_0 \left(\frac{UT - SV}{S^2 + T^2} \right) \tag{15}$$

where G is the complex moment of magnetization, u and v are the pure absorption and pure dispersion line shapes, respectively, and

$$S = \frac{p_A}{T_{2A}} + \frac{p_B}{T_{2B}} + \frac{\tau}{T_{2A}T_{2B}} - (\omega_A - \omega)(\omega_B - \omega) \tag{16}$$

$$U = 1 + (p_B/T_{2A} + p_A/T_{2B}) \tag{17}$$

$$T = (p_A\omega_A + p_B\omega_B - \omega) + \tau \left(\frac{(\omega_A - \omega)}{T_{2B}} + \frac{(\omega_B - \omega)}{T_{2A}} \right) \tag{18}$$

$$V = (p_B\omega_A + p_A\omega_B - \omega) \tag{19}$$

where p_A and p_B are the relative populations at sites A and B, respectively, and τ is the mean lifetime of the interaction defined by,

$$\tau = \frac{\tau_A \tau_B}{\tau_A + \tau_B} \tag{20}$$

The quantities ω_A and ω_B are the resonance frequencies in radians per second at the two sites at a given temperature in the absence of exchange and T_{2A} and T_{2B} are the respective relaxation times at each site at a given temperature in the absence of exchange. If at a given temperature the lifetime τ is greater than $\sqrt{2}/(\pi\Delta\omega)$, where $\Delta\omega = |\omega_A - \omega_B|$, two separate resonances are observed for the two respective sites; if τ is less than $\sqrt{2}/(\pi\Delta\omega)$, only one population-averaged resonance is observed.

Since it was experimentally difficult and inconvenient in the case of coalescing lines to obtain a pure absorption mode signal, a phase correction was made and the observed line shape was fitted by the following equation:

$$V = u\sin\theta + v\cos\theta + c \qquad (21)$$

where θ is the phase correction parameter and c the base line adjustment parameter.

Spectra with C211, obtained at selected temperatures in pyridine, formamide, dimethylformamide, dimethylsulfoxide and water are shown respectively in Figures 18 to 22. Spectra with C221 obtained at selected temperatures in pyridine are shown in Figure 23. Spectra were analyzed by using the Fortran IV KINFIT program (108) based on a generalized weighted non-linear least-squares analysis. A more detailed derivation and subroutine EQN are given in Appendix III. Each spectrum was fitted with four parameters,

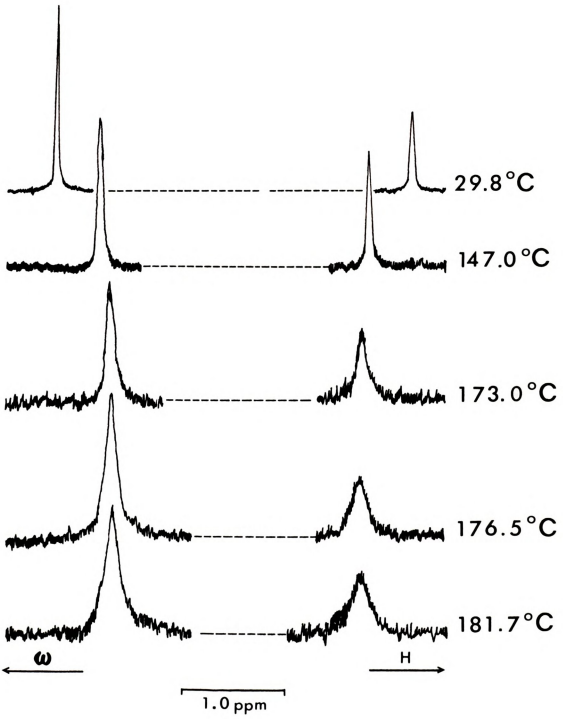

Figure 18. Lithium-7 NMR spectra of 0.50 M $LiClO_4$, 0.25 M C211 solution in pyridine at various temperatures.

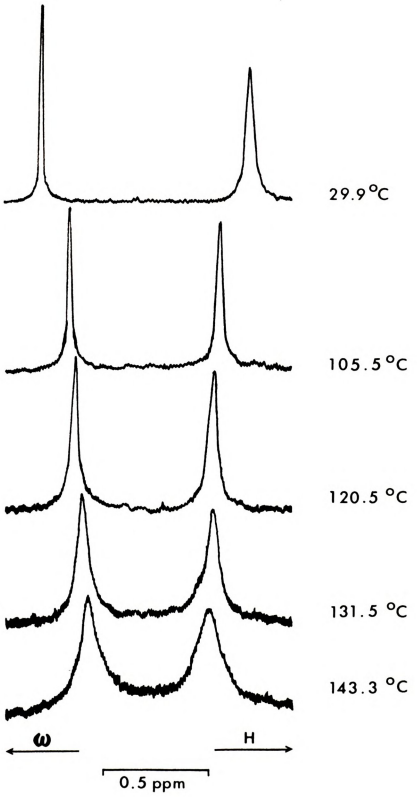

Figure 19. Lithium-7 NMR spectra of 0.50 M $LiClO_4$, 0.25 M C211 solution in formamide at various temperatures.

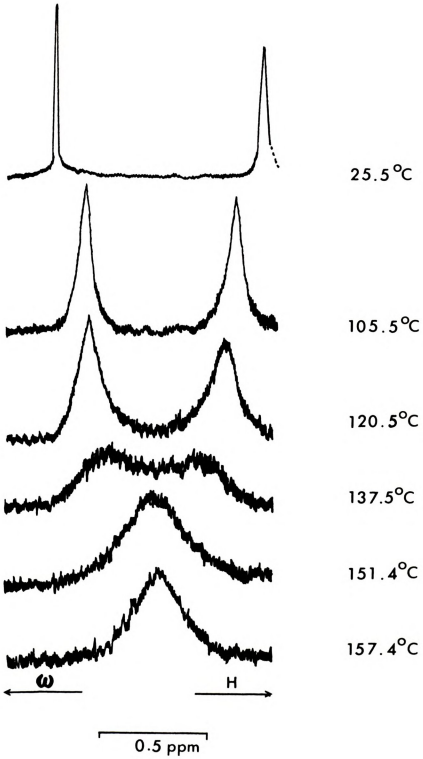

Figure 20. Lithium-7 NMR spectra of 0.50 M $LiClO_4$, 0.25 M C211 solution in dimethylformamide at various temperatures.

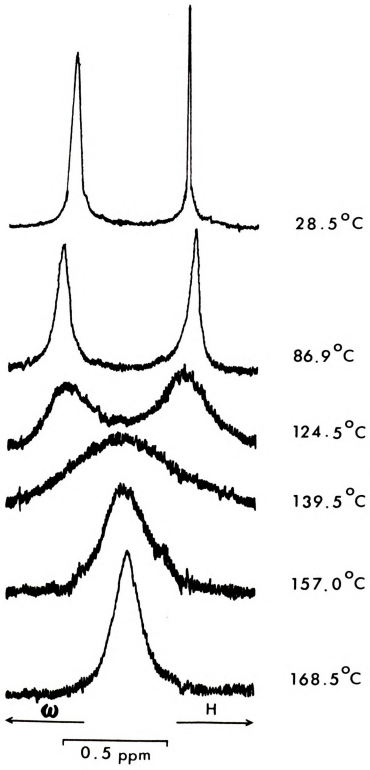

Figure 21. Lithium-7 NMR spectra 0.50 M $LiClO_4$, 0.25 M C211 solution in dimethylsulfoxide at various temperatures.

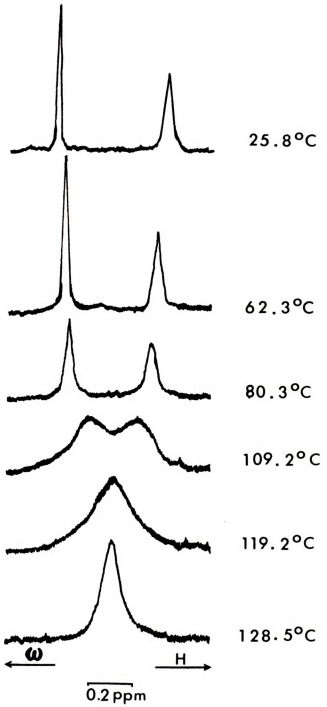

Figure 22. Lithium-7 NMR spectra of 0.50 M LiI, 0.25 M C2l1 solution in water at various temperatures.

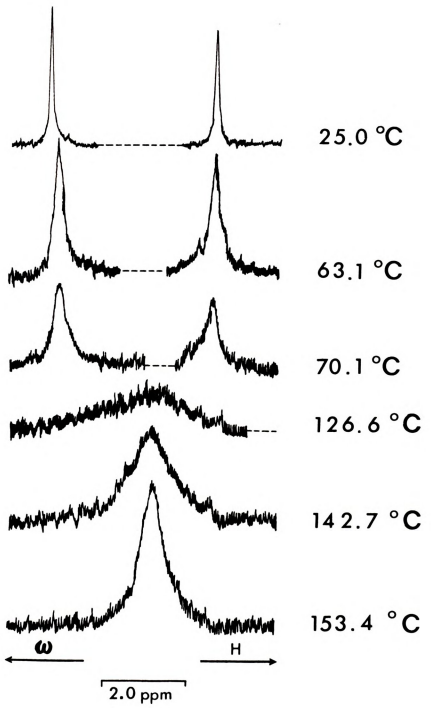

Figure 23. Lithium-7 NMR spectra of 0.50 M $LiClO_4$, 0.25 M C221 solution in pyridine at various temperatures.

the lifetime τ, the phase correction θ, the base line adjustment c and a normalization factor. A typical computer output (Figure 24) shows the fit of a spectrum ($LiClO_4$, C211) in formamide at 143.3°C.

No exchange is observed for the Li^+-C211 systems at room temperature. Measurable exchange, detected by the onset of broadening of both resonance lines, begins at higher temperatures, t_E which were found to be about 75°, 80°, 105°, 145°, and 85°C in dimethylsulfoxide, water, formamide, pyridine and dimethylformamide respectively. It was noted that ω_A and ω_B varied linearly with temperature relative to the lock frequency. The difference between the chemical shift (ppm) of the solvated ion A and that of the complexed ion B is a linear function of temperature as expressed by

$$\delta_A - \delta_B \equiv \Delta(\delta) = \Delta(\delta_o) - S(t-25) \qquad (22)$$

in which $\Delta(\delta_o)$ is $\delta_A - \delta_B$ at 25°C. The values of $\Delta(\delta_o)$ and S are given in Table VIII at temperatures higher than t_E, ω_A and ω_B were obtained by extrapolation. The validity of this extrapolation was verified in the case of the DMSO system by separate experiments on solutions which contained only A or B. The T_{2A} and T_{2B} values given in Table VIII were determined by measurement of the full width at half height of each resonance line and were found to be temperature independent. It should be noted that the cryptate

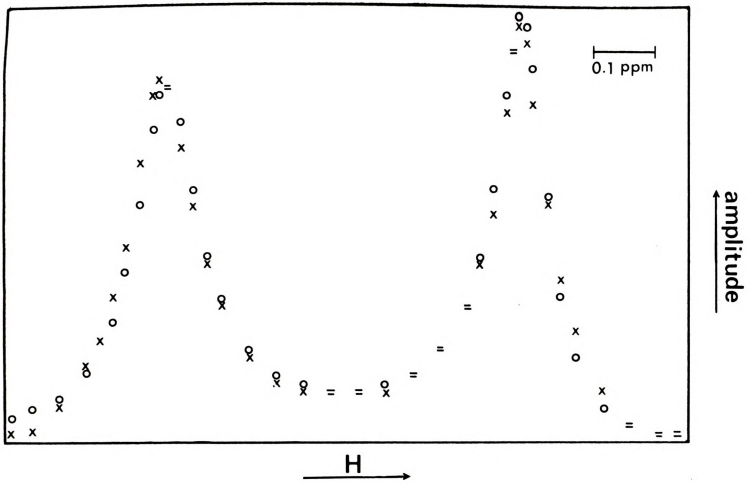

Figure 24. Computer fit of spectra obtained with 0.50 M $LiClO_4$, 0.25 M C2ll in formamide at 143.3°C. X means an experimental point, O means a calculated point, = means an experimental and calculated point are the same within the resolution of the plot.

Table VIII. Description of $\Delta(\delta)$ as a Function of Temperature.

$\Delta(\delta) = \Delta(\delta_o) + S(t - 25)$

$\Delta(\delta) = \delta_A - \delta_B$ at a given temperature t (^oC)

$\Delta(\delta_o) = \delta_A - \delta_B$ at 25^oC (A = solvated ion, B = complexed ion)

Solvent	Salt	Cryptand	$\Delta(\delta_o)$ ppm	S ppm/^oC	T_{2A} (sec)	T_{2B} (sec)
Pyridine	$LiClO_4$	211	3.425	-0.00696	0.796	0.637
Water	LiI	211	0.520	-0.00222	0.796	0.354
Dimethylsulfoxide	$LiClO_4$	211	-0.525	0.00181	0.909	0.374
Dimethylformamide	$LiClO_4$	211	0.999	-0.00364	1.061	0.455
Formamide	$LiClO_4$	211	1.010	-0.00370	0.909	0.374
Pyridine	$LiClO_4$	221	-3.986	-0.00746	0.707	0.637

resonance line is 2 to 3 times broader than that for the solvated ion. Therefore, the width of the cryptate resonance line cannot be entirely caused by field inhomogeneities.

In the case of the Li^+-C221 system in pyridine, ω_A, ω_B, T_{2A} and T_{2B} were measured by separate experiments since some exchange occurs at room temperature.

Activation energy plots, log k_b vs 1/T, are shown in Figure 25. Activation energies (E_a), rate constants (k_b), and values of $\Delta H_o^{\ddagger}$, $\Delta S_o^{\ddagger}$ and $\Delta G_o^{\ddagger}$ for the release of Li^+ from the cryptate are given in Table IX. A complete error analysis (123), including cross correlation terms which account for the coupling of parameters, (particularly evident between $\Delta H_o^{\ddagger}$ and $\Delta S_o^{\ddagger}$) was performed in all cases. Not surprisingly, $\Delta G_o^{\ddagger}$, which is directly determined from k_b, has the smallest standard deviation.

The accuracy of the determination of the activation energy depends upon the range of temperatures over which the exchange can be measured. For example, with the Li^+-C211 system in pyridine (Figure 18) the difference between the chemical shift of the solvated and the complexed lithium ion is 2.7 ppm, which is considerably larger than the shifts found in other solvents (0.5-1 ppm). Thus, for this system the exchange is observable over only a limited temperature range and coalescence could not be observed. Therefore, the activation energy could only be determined from the line broadening below the coalescence, which accounts for

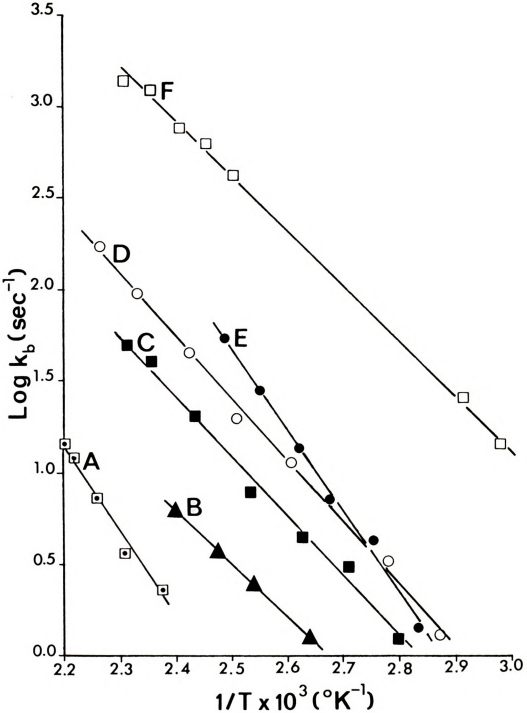

Figure 25. Log k_b vs 1/T plot for 0.50 M $LiClO_4$, 0.25 M C211 in (A) pyridine, (B) formamide, (C) dimethylformamide, (D) dimethylsulfoxide; (E) 0.50 M LiI, 0.25 M C211 in water, and (F) 0.50 M $LiClO_4$, 0.25 M C221 in pyridine.

Table IX. Exchange Rates and Thermodynamic Parameters of Lithium Cryptate Exchange in Various Solvents.

Solvent	DN[a]	ε[b]	E_a kcal mol^{-1}	$k_b \times 10^3$ sec^{-1} (298°K)	$\Delta H^{\ddagger}_o$ kcal mol^{-1}	$\Delta S^{\ddagger}_o$ $cal\,^{o}K^{-1}$ mol^{-1}	$\Delta G^{\ddagger}_o$ kcal mol^{-1} (298°K)
Cryptand 211							
Pyridine	33.1	12.3	19.6 (3.5)[c]	0.12 (0.24)	19.0 (3.4)	-12.5 (9.2)	22.7 (1.1)
Water	33.0	78.6	21.3 (1.2)	4.9 (2.0)	20.7 (1.1)	+ 0.4 (3.0)	20.6 (0.2_5)
Dimethylsulfoxide	29.8	45.0	16.1 (0.6)	23.2 (5.4)	15.5 (0.6)	-13.8 (1.4)	19.7 (0.1_4)
Dimethylformamide	26.6	36.1	16.0 (0.6)	13.0 (3.3)	15.4 (0.6)	-15.5 (1.4)	20.0 (0.1_5)
Formamide	24.0	111.0	14.1 (0.7)	7.4 (2.9)	13.5 (0.7)	-22.8 (1.8)	20.8 (0.2_3)
Cryptand 221							
Pyridine	33.1	12.3	13.5 (0.4)	1230 (196)	12.9 (0.4)	-14.9 (0.9)	17.9 (0.1)

[a] Gutmann Donor Number (38).

[b] Dielectric constant.

[c] Standard deviation.

the relatively large standard deviation. On the other hand, for the Li^+-C22l system in the same solvent (Figure 23), the exchange is observable over a large temperature range, 62.6°C to 159.4°C, and the activation energy can be determined with a higher accuracy.

The energies of activation for the release of Li^+ from the Li^+-C21l complexes in pyridine, water, dimethylsulfoxide, dimethylformamide and formamide, seem to be determined by the donicity of the solvent as expressed by the Gutmann donor number (38), rather than the dielectric constant. The activation energies vary from 14.1 kcal mol^{-1} in formamide (DN = 24) to 21.3 kcal mol^{-1} in water (DN = 33.0). By contrast, Shchori, et al. (121), found that the (smaller) activation energies for the release of Na^+ from several 18-crown-6 complexing agents were independent of the solvent used. However, two of the three solvents used, methanol and dimethylformamide have the same donicity, while that of the third solvent, dimethylethane, is not known.

We expect that the net energy required to transfer Li^+ from the cryptate to the solvent should decrease with increasing donicity of the solvent since this scale is a good measure of the primary solvation energy. The solvation energy of the cryptate and the secondary solvation energy of the lithium ion both depend primarily upon the dielectric constant of the solvent and change in the same direction from solvent to solvent.

Since the activation energy increases with increasing donicity, opposite to the overall energy change, the transition state must involve substantial ionic solvation. The energy profile is illustrated schematically in Figure 26. The solid line represents the complexation path of Li^+-C21l in a poor donor solvent (S_2) and the dashed line in a good donor solvent (S_1) with reverse activation energies of E_{a_1} and E_{a_2}, respectively, ($E_{a_1} > E_{a_2}$). In the same solvent, for example S_2, the energy level of the 22l cryptate will be higher than for the cryptate 2ll because of the better fit of the lithium ion in the C2ll cavity. On the otherhand if the transition state is similar to the solvated lithium ion, its energy should not depend strongly upon the cryptand used. The energy of activation for Li^+-C22l (E_{a_3}) is lower than that for Li^+-C21l (E_{a_2}) in pyridine, 13.5 and 19.6 kcal mol^{-1}, respectively.

Although E_a, and hence $\Delta H_o^{\ddagger}$, are very sensitive to the solvent used, the values of $\Delta G_o^{\ddagger}$ (298°K) are nearly independent of solvent. Changes in $\Delta H_o^{\ddagger}$ are compensated for by corresponding changes in $\Delta S_o^{\ddagger}$, a not uncommon occurrence (124).

Using the formation constant of the Li^+-C21l cryptate in water determined by Lehn and coworkers (80), log K = 5.3, we can calculate the rate constant for the forward reaction, $k_f = Kk_b = 0.98 \times 10^3$ sec^{-1} for Li^+-C21l in water.

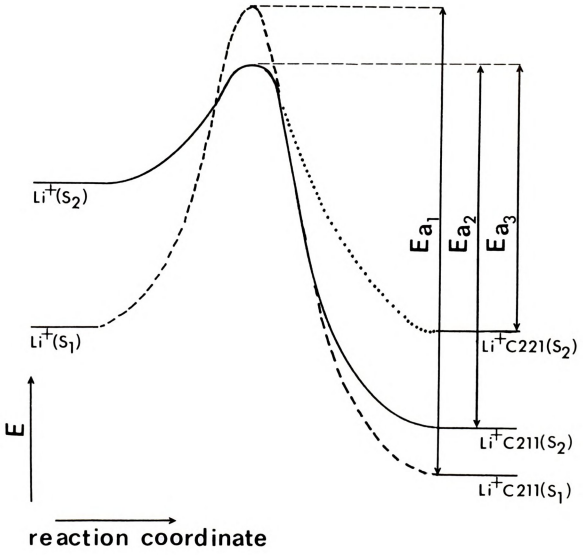

Figure 26. Schematic representation of the complexation of lithium ion by cryptands 211 and 221. S_1 represents a good donor solvent, S_2 a poor one.

B. FAR INFRARED AND RAMAN STUDY OF LITHIUM AND SODIUM CRYPTATES IN NONAQUEOUS SOLVENTS

1. Introduction

Far infrared spectroscopy has been used extensively (6-17) for the investigations of the motion of alkali metal cations relative to their immediate environment. In general, variations of the cation's motional frequencies in solution are expected to occur with variations in the immediate environment of the cation, and are indicative of interactions occurring in solutions. For example, cation-dependent frequencies can be either dependent or independent of the anion, indicating the presence or absence of the anion in the first solvation sphere of the cation, i.e., formation of the contact ion pair.

When an alkali ion is complexed by a macrocyclic polyether, the ligand insulates it from the medium and a cation-ligand, rather than cation-solvent vibration is observed. Risen and coworkers (69) investigated the far infrared spectra of the sodium and potassium-dibenzo-18-crown-6 systems in several solvents and found a band whose frequency was solvent independent.

2. Results and Discussion

a. Salts in solution. Far infrared spectra (100-500 cm^{-1}) of sodium salts ($NaBPh_4$ and NaI) in pyridine, DMSO and nitromethane and of lithium salts in nitromethane,

pyridine and acetonitrile are represented in Figures 27 and 28 respectively. Frequencies of the major far infrared bands, observed in the 100-500 cm^{-1} region, are reported in Table X.

For sodium ion solutions in pyridine and DMSO, anion independent and solvent dependent bands are observed at 180 cm^{-1} in pyridine and at 205 cm^{-1} in DMSO. These bands represent the vibrations of the sodium cation in a solvent cage (9-17). Pyridine and DMSO are solvents of high donicity and no significant concentration of contact ion pairs is present in these solutions. In nitromethane, a poor donor solvent, an anion dependent band is observed at 135 cm^{-1} for $NaBPh_4$ and at 148 cm^{-1} for $NaPF_6$. The anion dependence of the band frequency indicates significant anion participation in the near-neighbor environment of the cation.

For lithium salts in acetonitrile and pyridine, cation dependent bands are observed at 381 cm^{-1} and 387 cm^{-1}, respectively, due to the solvated cation. In nitromethane solutions the frequency of the lithium ion vibration is strongly anion-dependent. The bands are found at 358 cm^{-1} for $LiClO_4$ and 330 cm^{-1} for LiI. The 420 cm^{-1} band in pyridine is interpreted to be an activated complexed pyridine band (16). The other bands, reported in Table X, are due to solvent or internal vibration modes.

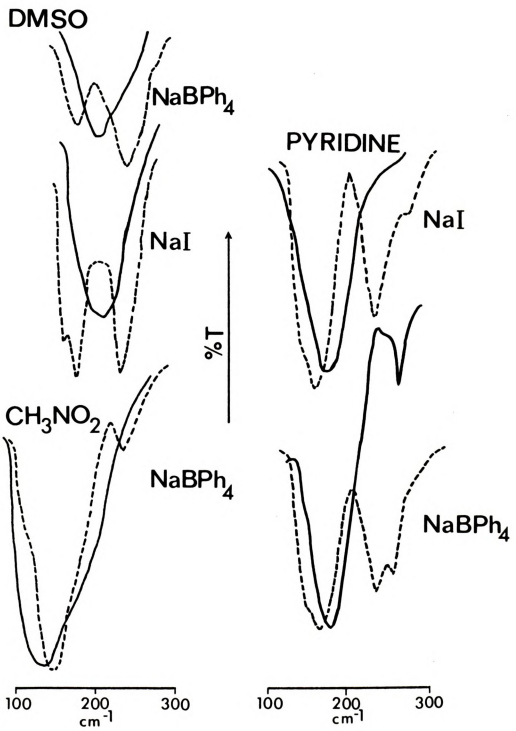

Figure 27. Far infrared spectra of nitromethane, pyridine and DMSO solutions of Na^+X^- salts (X^- = BPh_4^- and I^-) (solid lines) and of analogous 222 cryptates (dashed lines).

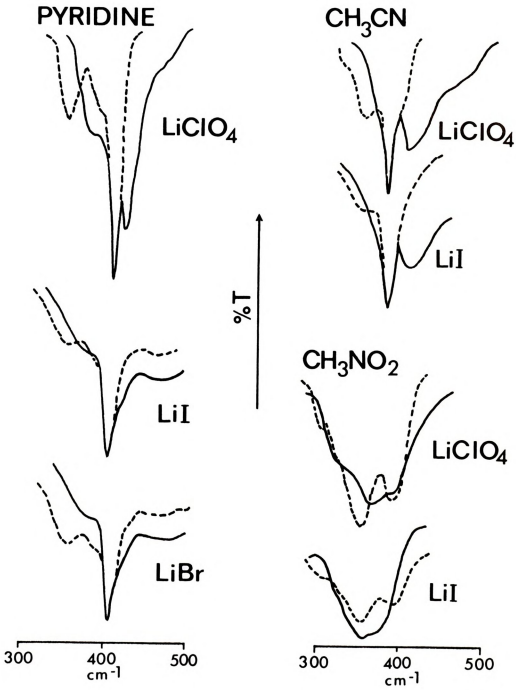

Figure 28. Far infrared spectra of nitromethane, pyridine and acetonitrile solutions of Li^+X^- salts (X^- = ClO_4^- and I^-) (solid lines) and of analogous 211 cryptates (dashed lines).

Table X. Far Infrared Bands of Sodium and Lithium Salts in Various Solvents.

Salt	Conc M	Solvent	Band Frequencies		
$NaPF_6$	0.25	CH_3NO_2	148(vs)	281(w)	480*(vs)
$NaBPh_4$	0.50	CH_3NO_2	135(vs)	281(w)	480*(vs)
	0.50	Pyridine	182(vs)	256(w)	407*(vs)
	0.50	DMSO	206(vs)	334*(vs)	382*(vs)
NaI	0.50	Pyridine	178(vs)	407*(vs)	
	0.50	DMSO	205(vs)	334*(vs)	382*(vs)
$LiClO_4$	0.60	CH_3NO_2	358$^+$(vs)	388$^+$(w)	480*(vs)
	0.50	CH_3CN	381*(vs)	405(vs)	
	0.60	Pyridine	387$^+$(w)	407*(vs)	422(s)
LiI	0.30	CH_3NO_2	330(vs)	480*(vs)	
	0.50	CH_3CN	381*(vs)	405(vs)	
	0.50	Pyridine	386$^+$(s)	407*(vs)	418$^+$(s)
LiBr	0.50	Pyridine	380$^+$(s)	407*(vs)	418$^+$(s)

w - weak, m - medium, s - strong, vs - very strong

*solvent band

$^+$partially resolved

b. Cryptates in Solution. The far infrared spectra (100-500 cm^{-1}) of Na^+-C222 complexes in pyridine, DMSO, and nitromethane and of Li^+-C211 complexes in pyridine, acetonitrile and nitromethane are shown in Figures 27 and 28, respectively. The frequencies of major far infrared bands observed in this region for the sodium and lithium cryptates are given in Table XI.

The addition of cryptand to a sodium or lithium ion solution results in the disappearance of the cation-solvent vibrational band and the appearance of a new band whose frequency is both anion and solvent independent. For example, the Na^+-C222 system in pyridine, DMSO and nitromethane has a new band at 234±2 cm^{-1} in all three solvents. Similarly, the Na^+-C221 complex has a solvent and anion independent band at 218±1 cm^{-1}, the Li^+-C221 complex, at 243±3 cm^{-1} and that of the Li^+-C211 complex, at 348±1 cm^{-1}.

The substitution of ^6Li for ^7Li in pyridine solutions changes the frequency of the Li^+-C211 band from 348 cm^{-1} to 369 cm^{-1} confirming that the vibration involves the lithium ion (Figure 29 and Table XI).

These results are analogous to those of Tsatsas et al. (69) with the crown ethers. They indicate that the alkali metal ions are completely enclosed in the cryptand cavity and the new bands indicate the vibrations of the cations inside the cavity. It is interesting to note that the frequencies of sodium ion motion in the C222 and C221 cryptands are at higher frequency than those for the simple

Table XI. Frequencies (cm^{-1}) of the Major Far Infrared Bands for Cryptates in Various Solvents.

Cryptate	Conc (M)	Solvent	Band Frequencies (cm^{-1})				
Na^+-C222 BPh_4^-	0.50	CH_3NO_2	145(vs)	234(s)	281(w)	480*(vs)	
	0.50	Pyridine	163(vs)	236(s)	257(w)	407*(vs)	
	0.25	DMSO	176(vs)	237(s)	334*(vs)	382*(vs)	
	0.25	DMSO-d_6	172(vs)	235(s)	256(w)	310*(vs)	343*(vs)
Na^+-C222 I^-	0.15	Pyridine	160(vs)	234(s)	360(s)	407*(vs)	
	0.25	DMSO	174(vs)	232(s)	279(s)	334*(vs)	382*(vs)
Na^+-C221 BPh_4^-	0.45	Pyridine	180(vs)	218(vs)	260(w)	407*(vs)	
Na^+-C221 I^-	0.60	DMSO	178(vs)	217(vs)	334*(vs)	382*(vs)	
Li^+-C211 ClO_4^-	0.80	CH_3NO_2	348(vs)	385(s)	480*(vs)		
	0.60	CH_3CN	348(vs)	381*(s)			
	0.50	Pyridine	348(vs)	385(s)	407*(vs)		
$^6Li^+$-C211 ClO_4^-	0.50	Pyridine	370(vs)	407*(vs)			
$^6Li^+$-C211 ClO_4^-	0.50	CH_3NO_2	368(vs)	405(s)	480*(vs)		
Li^+-C211 I^-	0.35	CH_3NO_2	348(vs)	391(s)	480*(vs)		
	0.15	CH_3CN	350(vs)	381*(s)			
	0.20	Pyridine	350(vs)	385+(s)	407*(vs)		

Table XI. Continued

Cryptate	Conc (M)	Solvent	Band Frequencies (cm^{-1})		
Li^{+}-C211 Br^{-}	0.50	Pyridine	350(vs)	386^{+}(s)	407*(vs)
Li^{+}-C221 ClO_4^{-}	0.60	Pyridine	240(m)	407*(vs)	
Li^{+}-C221 I^{-}	0.50	DMSO	246(m)	334*(vs)	382*(vs)

w - weak, m - medium, s - strong, vs - very strong
*solvent band
$^{+}$partially resolved

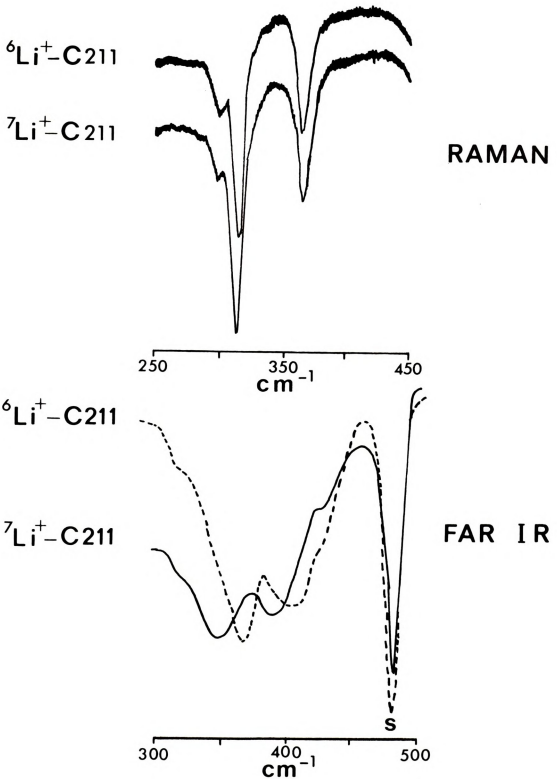

Figure 29. Raman and far infrared spectra of ^{6}Li-C211 and ^{7}Li-C211 cryptates in nitromethane solution. S - solvent band.

sodium salt solutions in the same solvents while the frequencies of lithium motion in C211 and C221 are generally at a lower frequency than those for the simple lithium salt solutions in the solvent (Figure 30). The only exception is the frequency of the lithium iodide vibration in nitromethane where the salt exists largely as a contact ion pair.

The fact that these frequencies reflect the strength of interaction of the alkali ion with the cryptand is illustrated by the difference in the vibrational frequency between Li^+-C221 and Li^+-C211 complexes which are observed at 243 and 348 cm^{-1}, respectively. In the latter case, the Li^+ ions fit exactly into the cryptand cavity and the more rigid structure results in a higher vibrational frequency.

The other interesting feature of cryptate far infrared spectra is the appearance of another band whose frequency is solvent dependent but anion independent. Such bands are found at 161 cm^{-1}, 176 cm^{-1} and 145 cm^{-1} for Na^+-C222 in pyridine, dimethylsulfoxide and nitromethane, respectively, and at 388 cm^{-1} and 385 cm^{-1} for Li^+-C211 in nitromethane and pyridine, respectively. Substitution of DMSO by d_6-DMSO shifts the 176±1 cm^{-1} band to 172±1 cm^{-1} clearly indicating the participation of the solvent in the observed vibration. Such a band is not observed for Li^+-C211 complex in acetonitrile solution; it is possibly masked by the strong 381 cm^{-1} solvent band of acetonitrile. It seems reasonable to assume that the observed band can be assigned

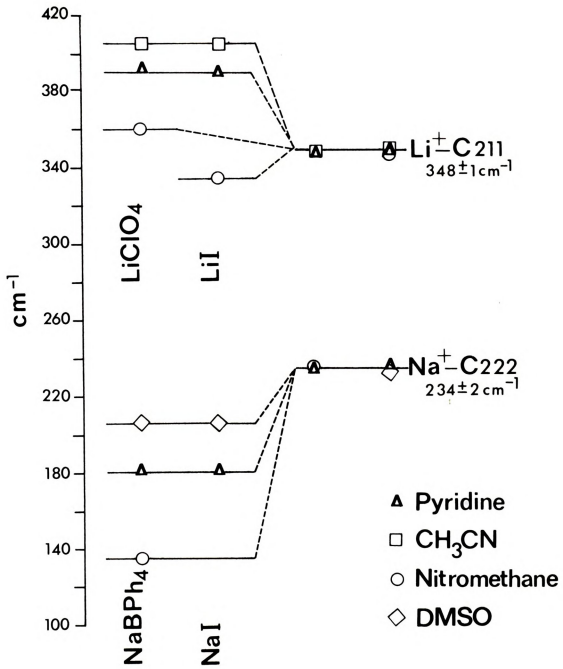

Figure 30. Comparison of ion motion band frequencies for sodium and lithium salts and their 222 and 211 cryptates respectively in pyridine, acetonitrile, nitromethane, dimethylsulfoxide solutions.

to the vibration of solvent molecules which are in the first solvation shell of the cryptate moiety.

Raman spectra were obtained for the Li^+-C211 cryptates in pyridine and nitromethane solutions and it was found that the 348 cm^{-1} infrared band is Raman-inactive. The data are shown in Figure 29 and Table XII. Two strong bands, however, are observed at 367 cm^{-1} and 312 cm^{-1} in both solvents. These bands cannot be assigned to a vibration of the cryptate or to a displaced solvent band. Their frequencies are unaffected by isotopic substitution of ^6Li for ^7Li (Figure 29), and, therefore, they cannot be a displaced cryptate vibration. We feel that they represent activated cryptand vibrations.

The fact that the lithium-cryptand vibration is Raman-inactive allows some speculation on the nature of the complexation interaction. It was pointed out by Edgell and coworkers (8) that the far infrared cation-solvent vibrational bands are Raman-inactive, indicating the electrostatic nature of the interaction. Since the same selection rules apply to the cation-cryptand vibration, it seems reasonable to conclude that in this case the cation-ligand interaction is predominantly electrostatic in nature.

Table XII. Raman Bands of Li^+-C21l Complexes in Pyridine and Nitromethane Solutions

Pyridine

Solute	Conc (M)	Observed Bands(cm^{-1}) in the 150 to 450 cm^{-1} region				
C21l	0.50	406[a]±1	378[a]±1	325[b]±3		
LiBr	0.55	406[a]±1	378[a]±2			
Li^+-C21l Br^-	0.50	406[a]±1	378[a,c]±2	366 ±2	311±1	298[a,c]±3

Nitromethane

C21l	0.45	320[b]±5				
Li^+-C21lClO_4^-	0.55	367 ±1	312±1	298[c]±2		
$^7Li^+$-C21l ClO_4^-	0.60	367 ±1	313±1	299[c]±2		

[a]Solvent band.

[b]Broad band.

[c]Partially resolved.

C. CONCLUSIONS AND SUGGESTIONS FOR FURTHER STUDIES

Lithium-7 NMR has been applied to the study of ionic interactions of lithium in various solvents, to the determination of complex formation constants of weak and relatively strong complexes, and, furthermore, to the investigation of the kinetics of the complexation. Other techniques, such as ^{35}Cl NMR, laser Raman spectroscopy and far infrared spectroscopy have been used to obtain complementary and additional information in order to more fully understand the role of the solvent in chemical processes.

In light of the studies accomplished, the following suggestions can be made for further investigations:

1. Study of the variation of the ^{7}Li chemical shift as a function of concentration in the low concentration range; (<0.01 M). The limiting chemical shift could then be reached even in solvents where ion pairs are formed. Pulse technique will have to be used, and the water content of each solution will have to be kept at an extremely low level so the ^{7}Li chemical shift will not be affected.

2. Investigation of the kinetics of the formation of Li^{+}-C211 complexes in low donor solvents to see if the same trend is observed between the activation energies and the donicity of the solvent in which the complexation is carried out.

3. Investigation of the kinetics of the complexation of Na^{+}-C221 in various solvents for which the cation-

cryptand cavity fit is analogous to the fit between Li^+ and C211.

4. Determination of complex formation constants of cryptates in various solvents. Nuclear Magnetic Resonance technique could be used by either the direct method in the cases of a fast exchange and weak to relatively strong complexes, or by stepwise method, carrying out competitive complexation reactions.

APPENDICES

APPENDIX I

LITHIUM-7 CHEMICAL SHIFTS VS 4.0 M AQUEOUS $LiClO_4$ of VARIOUS LITHIUM SALTS IN VARIOUS SOLVENTS.

ACETONITRILE

$LiClO_4$	Conc (M)	ppm	LiBr	Conc (M)	ppm
	0.500	2.17		0.503	1.52
	0.250	2.29		0.376	1.62
	0.123	2.33		0.251	1.59
	0.062	2.49		0.126	1.67
	0.031	2.55		0.075	1.72
	0.016	2.60		0.037	1.77
				0.025	1.87
$LiBPh_4$	0.509	1.75	LiI_3	0.501	2.55
	0.254	1.99		0.251	2.59
	0.127	2.19		0.125	2.71
	0.064	2.35		0.063	2.72
	0.032	2.46		0.031	2.75
	0.016	2.49		0.016	2.76
LiI	0.500	2.31			
	0.250	2.44			
	0.125	2.53			
	0.062	2.60			
	0.031	2.64			
	0.016	2.67			

NITROMETHANE

$LiClO_4$	Conc (M)	δ_{ppm}	LiI_3	Conc (M)	δ_{ppm}
	3.50*	0.90		0.506	0.07
	3.00	0.93		0.253	0.20
	2.50	0.91		0.126	0.30
	2.00	0.89		0.063	0.34
	1.50	0.88		0.032	0.36
	1.00	0.85		0.016	0.38
	0.510	0.82			
	0.300	0.78	LiI	0.250*	-0.63
	0.200	0.74		0.125	-0.58
	0.100	0.67		0.062	-0.48
	0.082	0.65		0.031	-0.40
	0.061	0.62		0.016	-0.34
	0.030	0.52			
	0.020	0.47			
	0.014	0.41			
$LiBPh_4$	0.250*	0.40			
	0.125	0.39			
	0.062	0.37			
	0.031	0.35			
	0.016	0.34			

*Solubility limit

DIMETHYLSULFOXIDE

$LiClO_4$	Conc (M)	δ_{ppm}	LiBr	Conc (M)	δ_{ppm}
	0.526	1.07		0.680	1.10
	0.394	1.05		0.511	1.08
	0.263	1.03		0.341	1.12
	0.131	1.05		0.171	1.10
	0.078	1.03		0.102	1.12
	0.058	1.03		0.068	1.07
	0.026	1.07		0.034	1.12
$LiBPh_4$	0.497	1.05	LiI	0.500	1.00
	0.248	1.03		0.250	1.03
	0.124	1.06		0.125	1.04
	0.062	1.06		0.062	1.04
	0.031	1.05		0.031	1.05
	0.016	1.06		0.016	0.96

1,2-DICHLOROETHANE

LiCl	0.500	0.90			
	0.250	0.93	$LiBPh_4$	Conc (M)	δ_{ppm}
	0.125	0.97		0.496	1.18
	0.062	1.02		0.248	0.82
	0.031	1.03		0.124	0.80
	0.016	1.04			

METHANOL

$LiClO_4$	Conc (M)	δ_{ppm}	LiCl	Conc (M)	δ_{ppm}
	6.50*	0.69		0.500	0.52
	6.00	0.65		0.250	0.56
	5.50	0.63		0.125	0.58
	5.00	0.61		0.062	0.59
	4.29	0.59		0.031	0.59
	3.75	0.59		0.016	0.59
	3.33	0.57			
	2.14	0.57	LiBr	0.500	0.54
	1.66	0.58		0.250	0.57
	0.50	0.57		0.125	0.58
	0.25	0.58		0.032	0.59
	0.125	0.59			
	0.062	0.58			
	0.031	0.57			
	0.016	0.57	LiI	0.500	0.53
				0.250	0.56
$LiBPh_4$	0.250	0.59		0.125	0.47
	0.125	0.60		0.062	0.57
	0.062	0.63		0.031	0.58
	0.016	0.64		0.016	0.58

*Solubility limit

ACETIC ACID			PROPYLENE CARBONATE		
$LiClO_4$	Conc (M)	δ_{ppm}	$LiClO_4$	Conc (M)	δ_{ppm}
	0.490	0.15		0.500	0.47
	0.245	0.11		0.250	0.54
	0.122	0.08		0.125	0.57
	0.061	0.05		0.062	0.60
	0.031	0.04		0.031	0.62
				0.016	0.63
$LiBPh_4$	0.505	0.01	$LiBPh_4$	0.500	0.48
	0.252	0.02		0.250	0.51
	0.126	0.02		0.125	0.55
				0.062	0.57
				0.016	0.60
LiI	0.500	-0.02	LiBr	0.500	0.21
	0.250	+0.00(4)		0.250	0.30
	0.125	+0.03		0.125	0.37
	0.062	+0.04		0.062	0.44
	0.031	+0.06		0.031	0.51
				0.016	0.55
LiI_3	0.500	-0.12	LiI	0.500	0.26
	0.250	-0.05		0.125	0.44
	0.125	-0.03		0.062	0.51
	0.062	-0.01		0.031	0.56
	0.031	+0.01		0.016	0.61
	0.016	+0.02			

DIMETHYLFORMAMIDE

$LiClO_4$	Conc (M)	δ_{ppm}	LiBr	Conc (M)	δ_{ppm}
	0.500	-0.41			
	0.250	-0.41		0.500	-0.45
	0.125	-0.42		0.250	-0.43
	0.062	-0.42		0.125	-0.43
	0.031	-0.42		0.062	-0.42
	0.016	-0.42		0.031	-0.41
				0.016	-0.41
$LiBPh_4$	0.503	-0.46			
	0.251	-0.44	LiI	0.500	-0.42
	0.125	-0.42		0.250	-0.41
	0.062	-0.41		0.125	-0.40
	0.031	-0.39		0.062	-0.40
	0.016	-0.37		0.031	-0.40
LiCl	0.500	-0.60			
	0.250	-0.57			
	0.125	-0.55			
	0.062	-0.52			
	0.031	-0.50			
	0.016	-0.49			

TETRAHYDROFURAN

$LiClO_4$	Conc (M)	δ_{ppm}	LiBr	Conc (M)	δ_{ppm}
	2.00*	0.64		1.124	-0.76
	1.50	0.66		0.562	-0.71
	1.00	0.66		0.281	-0.69
	0.44	0.64		0.140	-0.69
	0.22	0.63		0.070	-0.63
	0.110	0.63		0.035	-0.60
	0.055	0.61		0.018	-0.60
	0.028	0.63			
	0.014	0.61	LiI	Conc (M)	ppm
$LiBPh_4$	0.510	0.62		0.500	-0.66
	0.255	0.60		0.250	-0.67
	0.128	0.58		0.125	-0.69
				0.062	-0.69
LiCl	0.500*	-0.53		0.031	-0.67
	0.250	-0.53		0.016	-0.58
	0.125	-0.52			
	0.062	-0.52	LiI_3	0.500	0.50
	0.031	-0.50		0.250	0.55
	0.016	-0.48		0.125	0.60
				0.062	0.61
				0.031	0.60
				0.016	0.58

*Solubility limit

ACETONE

$LiClO_4$	Conc (M)	δ_{ppm}	LiBr	Conc (M)	δ_{ppm}
				0.418	-1.47
	3.50	-0.76		0.314	-1.51
	4.00	-0.85		0.209	-1.51
	3.00	-0.89		0.105	-1.54
	2.50	-0.90		0.063	-1.53
	2.00	-1.00		0.042	-1.53
	1.00	-1.05		0.021	-1.51
	0.50	-1.06	LiI	0.500	-1.46
	0.25	-1.07		0.250	-1.43
	0.125	-1.14		0.125	-1.43
	0.062	-1.14		0.062	-1.43
	0.031	-1.18		0.031	-1.43
	0.016	-1.24		0.016	-1.44

WATER

$LiBPh_4$	0.504	-1.11			
	0.252	-1.18	LiI	Conc (M)	δ_{ppm}
	0.126	-1.23		4.00	0.000
	0.062	-1.25		1.00	0.064
	0.031	-1.31		0.25	0.060
	0.016	-1.31		0.06	0.081
				0.015	0.086

TETRAMETHYLGUANIDINE

$LiClO_4$	Conc (M)	δ_{ppm}	LiI	Conc (M)	δ_{ppm}
	0.500	-0.44		0.500	-0.78
	0.250	-0.44		0.250	-0.74
	0.125	-0.43		0.125	-0.70
	0.062	-0.41		0.062	-0.69
	0.031	-0.41		0.031	-0.68
$LiBPh_4$	0.500	-0.54	LiI_3	0.500	-0.76
	0.250	-0.55		0.250	-0.69
	0.125	-0.55		0.125	-0.64
	0.062	-0.58		0.062	-0.64
	0.031	-0.58		0.031	-0.63
				0.016	-0.65
LiCl	0.500	-0.80			
	0.250	-0.77			
	0.125	-0.74			
	0.062	-0.71			
	0.031	-0.71			
	0.016	-0.71			

PYRIDINE

$LiClO_4$	Conc (M)	δ_{ppm}	LiBr	Conc (M)	δ_{ppm}
	0.500	-2.01		0.500	-2.88
	0.250	-2.07		0.250	-2.93
	0.125	-2.12		0.125	-2.96
	0.062	-2.13		0.062	-2.98
	0.031	-2.17		0.031	-3.02
	0.016	-2.22		0.016	-3.06
$LiBPh_4$	0.498	-2.41	LiI	0.500	-2.82
	0.249	-2.43		0.250	-2.78
	0.124	-2.43		0.062	-2.74
	0.062	-2.47		0.031	-2.70
	0.031	-2.47		0.016	-2.67
	0.016	-2.47			
LiCl	0.500	-2.68			
	0.250	-2.75			
	0.125	-2.79			
	0.062	-2.84			
	0.031	-2.84			
	0.016	-2.86			

APPENDIX II

DETERMINATION OF COMPLEX FORMATION CONSTANTS BY THE NMR TECHNIQUE, DESCRIPTION OF COMPUTER PROGRAM KINFIT AND SUBROUTINE EQUATION.

Let's consider the following equilibrium for a one to one complex,

$$M + L \underset{k_b}{\overset{k_f}{\rightleftharpoons}} ML \tag{23}$$

with the concentration formation constant K

$$K = C_{ML} \; / \; C_M \cdot C_L \tag{24}$$

C, stands for concentration.

The observed chemical shift of M (δ_{obs}) is a mass average of the characteristic chemical shift of M at each site (M in the bulk solution, and M complexed), assuming that a fast exchange occurs between these two sites with respect to the NMR time scale.

$$\delta_{obs} = X_M \delta_M + X_{ML} \delta_{ML} \tag{25}$$

Where:

δ_M is the characteristic chemical shift for M in the bulk solution, δ_{ML} is the characteristic chemical shift for M complexed (ML), X_M is the fraction of M ($C_M/(C_M + C_{ML})$),

X_{ML} is the fraction of ML ($C_{ML}/(C_M + C_{ML})$), then

$$\delta_{obs} = X_M\delta_M + (1-X_M)\delta_{ML}$$

$$\delta_{obs} = X_M(\delta_M-\delta_{ML}) + \delta_{ML} \qquad (26)$$

$C_M^t = C_M + C_{ML}$ (the analytical concentration of M) (27)

$$\delta_{obs} = \frac{C_M}{C_M^t}(\delta_M-\delta_{ML}) + \delta_{ML} \qquad (28)$$

$C_L^t = C_{ML} + C_L$ (the analytical concentration of L) (29)

$$C_L = C_L^t - C_{ML}$$

using (27) and (29), $C_L = C_L^t - (C_M^t - C_M)$

$$K = \frac{C_M^t - C_M}{(C_M)(C_L^t - C_M^t + C_M)} \qquad (30)$$

C_M is solved in (30)

$C_M(C_L^t - C_M^t + C_M)K = C_M^t - C_M$

$KC_M^2 + (KC_L^t - KC_M^t + 1)C_m - C_M^t = 0$

$$C_M = \frac{-(KC_L^t - KC_M^t + 1) \pm \sqrt{(KC_L^t - KC_M^t + 1)^2 + 4KC_M^t}}{2K}$$

the positive root is

$$C_M = \frac{(KC_M^t - KC_L^t - 1) + \sqrt{K^2C_L^{t2} + K^2C_M^{t2} - 2K^2C_L^tC_M^t + 2KC_L^t + 2KC_M^t + 1}}{2K} \qquad (31)$$

Substitution of C_M from (31)' in Equation (28)

$$\delta_{obs} = \left[(KC_M^t - KC_L^t - 1) + \sqrt{K^2C_L^{t2} + K^2C_M^{t2} - 2K^2C_L^tC_M^t + 2KC_L^t + 2KC_M^t + 1}\right] \left[(\delta_M - \delta_{ML})/2C_M^tK\right] + \delta_{ML} \qquad (32)$$

We assume a constant value for δ_M and that δ_{ML} and K are unknown. In order to fit the calculated shift (the right hand side of Equation (32)) to the observed chemical shift, the program may vary the values of δ_{ML} and K. Hence, the number of unknowns, NOUNK, equals two as does the number of variables, NOVAR.

The first card contains the number of experimental points (columns 1-5 (F.15)), the maximum number of iterations allowed (columns 10-15 (F.15)), the number of constants (columns 36-40 (F.15)) and the maximum value of (Δ parameter/parameter) for convergence to be assumed (0.0001 works well) in columns 41-50 (F10.6). The second data card contains any title the user desires. The third data card contains the value of CONST(1) (C_M^t) columns 1-10 (F10.6) in M, CONST(2) (δ_M) columns 11-20 (F10.6) other constants can be listed on columns 21-30, 31-40, etc. The fourth data card contains

the initial estimates of the unknowns U(1) = δ_{ML} and U(2) = K, in columns 1-10 and 11-20 (F10.6), respectively. The fifth through N data cards contains XX(1) = C_M^t in columns 1-10 (F 10.6) variances on XX(1) in columns 11-20, XX(2) = the chemical shift at XX(1) in columns 31-40 (F 10.6) followed by the same parameters for the next data point. Each card may contain two data points. If no further data are to be analyzed the next card after the last data point(s) should be a blank card followed by a 6789 card. If more data sets are to be analyzed, the next card after the last data point(s) is the first data card of the next set. Generally the most common error using this program is an error MODE 4 in an address of the SQRTE subroutine. Usually this implies that the initial guess for K is quite inaccurate. If this becomes a problem, the argument of the square-root expression could be tested to make certain that it does not become negative. Before using this program, the user should see Reference (108), or the materials of CEM 883, Chemical Kinetics, to become familiar with the mode of operation and further application of program KINFIT.

```
FTN,
ATTACH(KINFIT,KINFIT)
LOAD(KINFIT)
LGO.
0000000000000000000000
      SUBROUTINE FON                                                    FON 1281
      COMMON KOUNT,ITAPE,JTAPE,IWT,LAP,XINCR,NOPT,NOVAR,NOUNK,X,U,ITMAX,FON 1282
     1WTX,TEST,I,AV,RESID,IAR,EPS,ITYP,XX,XTYP,DXI,FOP,FO,FU,P,ZL,TO,FON 1283
     2IGVAL,XST,T,DT,L,M,JJJ,Y,DY,VECT,NCST,CONST
      DIMENSION X(4,100), U(20), WTX(4,100), XX(4), FOP(100), FO(100), FON 1285
     1U(100), P(20,21), VECT(20,21), ZL(100), TO(20), EIGVAL(20), XST(10FON 1286
     20), Y(10), DY(10), CONST(16)                                      FON 1287
      GO TO (2,3,4,5,1), ITYP
    1 CONTINUE                                                          FON 1296
      ITAPE=A0                                                          FON 1300
      JTAPE=61
      WRITE (JTAPE,6)
    6 FORMAT(*0ETERMINATION OF FORMATION CONST BY LI 7 NMR*)
      NOUNK=2
      NOVAR=2
      RETURN
    2 CONTINUE
      A=(U(2)**2)*(XX(1)**2)
      B=(U(2)**2)*(CONST(1)**2)
      C=-2.0*(U(2)**2)*(XX(1))*CONST(1)
      D=2.0*(U(2))*(XX(1))
      E=2.0*(U(2))*(CONST(1))
      AA=(U(2))*(CONST(1))
      BB=-(U(2))*XX(1)
      CC=(CONST(2)-U(1))/(2.*(CONST(1))*(U(2)))
      S={{{AA*BB-1.)*SQRT(A*B+C*D+E*1.))*CC}*U(1)
      RFCT=S-XX(2)
      RETURN                                                            FON 1332
    3 CONTINUE
      RETURN
    4 CONTINUE
      RETURN
    5 CONTINUE
      RETURN
      END
0000000000000000003030
   40          20                    2.0001
0.01 MOLAR LICL04 MEGIMIDE
.0135     1.034
.45       4.0
.0029       1.0          1.000        25.0        .0061       1.0         .987        25.0
.0084       1.0          .987         25.0        .0139       1.0         .979        25.0
.0122       1.0          .971         25.0        .0155       1.0         .957        25.
.0174       1.0          .957         25.0        .0206       1.0         .953        25.0
.0293       1.0          .936         25.0        .0419       1.0         .910        25.0
.0503       1.0          .858         25.0        .0590       1.0         .863        25.0
.0712       1.0          .852         25.0        .0770       1.0         .846        25.0
.1021       1.0          .816         25.0        .1150       1.0         .781        25.0
.1324       1.0          .760         25.0        .1411       1.0         .745        25.0
.1516       1.0          .723         25.0        .1611       1.0         .713        25.0
.1695       1.0          .713         25.0        .1785       1.0         .700        25.0
.1901       1.0          .700         25.0        .2107       1.0         .670        25.0
.2202       1.0          .653         25.0        .2513       1.0         .637        25.0
.2819       1.0          .627         25.0        .2903       1.0         .618        25.0
.2977       1.0          .607         25.0        .3418       1.0         .584        25.0
.3592       1.0          .575         25.0        .3792       1.0         .562        25.0
.3944       1.0          .562         25.0        .4201       1.0         .541        25.0
.4349       1.0          .534         25.0        .4641       1.0         .524        25.0
.4668       1.0          .519         25.0        .5000       1.0         .509        25.0
.5281       1.0          .504         25.0        .5922       1.0         .476        25.0
.6192       1.0          .474         25.0        .6466       1.0         .472        25.0
.7156       1.0          .444         25.0        .7417       1.0         .438        25.0
.7707       1.0          .429         25.0        .8040       1.0         .421        25.0
.8234       1.0          .421         25.0        .8622       1.0         .421        25.0
.2561       1.0          .631         25.0
0000000000000000003030
0000000000000000000000
```

APPENDIX III

NMR LINE SHAPE ANALYSIS FOR TWO SITE EXCHANGE. DESCRIPTION OF COMPUTER PROGRAM AND SUBROUTINE EQN.

A. NMR LINE SHAPE ANALYSIS FOR TWO SITE EXCHANGE.

Definitions

$G \equiv$ complex moment of magnetization.

$A,B \equiv$ Respective sites.

$p_A, p_B \equiv$ Fractional population at site A and B. $(p_A + p_B = 1)$

T_{2A}, T_{2B} Transverse relaxation times of nuclei at the two sites, in the absence of exchange.

τ_A, τ_B Life time on site A and B at a given temperature.

ω_A, ω_B Chemical shift at site A and B in the absence of exchange.

γ Gyromagnetic ratio.

H_1 Radio frequency magnetic field

$M_{o(A,B)}$ Magnetization in the Z direction at both sites.

For two sites in the absence of exchange one can write (122):

$$\frac{dG_A}{dt} + \alpha_A G_A = -i\gamma H_1 M_{oA} \tag{33}$$

$$\frac{dG_B}{dt} + \alpha_B G_B = -i\gamma H_1 M_o B \tag{34}$$

where α_A and α_B are complex quantities defined by

$$\alpha_A = T_{2A}^{-1} - i(\omega_A - \omega) \tag{35}$$

$$\alpha_B = T_{2B}^{-1} - i(\omega_B - \omega) \tag{36}$$

Let's assume an exchange between site A and B following the two basic assumptions.

1. All nuclei remain in one site until they make a sudden rapid jump to another (nuclear precession during jump being neglected). Under these circumstances, it is clear that a nuclear exchange between positions of the same type will have no effect.

2. It will be assumed that while a nucleus is in A position, there is a constant probability τ_A^{-1} per unit time of its making a jump to a B position.

Fractional populations p_A and p_B are related to τ_A and τ_B by

$$p_A = \frac{\tau_A}{\tau_A + \tau_B}, \qquad p_B = \frac{\tau_B}{\tau_A + \tau_B}$$

Modified Bloch equations proposed by McConnell (125) are

$$\frac{dG_A}{dt} + \alpha_A G_A = - i\gamma H_1 M_{oA} + \tau_B^{-1} G_B - \tau_A^{-1} G_A \qquad (37)$$

$$\frac{dG_B}{dt} + \alpha_B G_B = - i\gamma H_1 M_{oB} + \tau_A^{-1} G_A - \tau_B^{-1} G_B \qquad (38)$$

Assuming a small radio frequency field H_1, for slow passage conditions we have:

$$\frac{dG_A}{dt} = \frac{dG_B}{dt} = 0 \qquad (39)$$

Also

$$M_{oA} = p_A M_o, \quad M_{oB} = p_B M_o$$

Solving (33) for G_A

$$\alpha_A G_A = - i\gamma H_1 M_{oA} + \tau_B^{-1} G_B - \tau_A^{-1} G_A \tag{40}$$

$$G_A = (-i\gamma H_1 M_{oA} + \frac{G_B}{\tau_B}) / (\alpha_A + \frac{1}{\tau_A}) \tag{41}$$

substitute equation (41) into (38) and solve for G_B

$$\alpha_B G_B = - i\gamma H_1 M_{oB} - \frac{-i\gamma H_1 M_{oA} + \frac{G_B}{\tau_B}}{(\alpha_A + \frac{1}{\tau_A})\tau_A} - \tau_B^{-1} G_B \tag{42}$$

$$G_B = \frac{(-i\gamma H_1 M_{oB} - \frac{i\gamma H_1 M_{oA}}{\alpha_A \tau_A + 1})(\tau_B)(\alpha_A \tau_A + 1)}{(\alpha_B \tau_B + 1)(\alpha_A \tau_A + 1) - 1} \tag{43}$$

and then from inspection

$$G_A = \frac{(-i\gamma H_1 M_{oA} - \frac{i\gamma H_1 M_{oB}}{\alpha_B \tau_B + 1})(\tau_A)(\alpha_B \tau_B + 1)}{(\alpha_A \tau_A + 1)(\alpha_B \tau_B + 1) - 1} \tag{44}$$

$G = G_A + G_B = u + iv$

$$G = \left[(-i\gamma H_1 M_{oA} - \frac{i\gamma H_1 M_{oB}}{\alpha_B \tau_B + 1})(\tau_A)(\alpha_B \tau_B + 1) + \right.$$

$$\left.(-i\gamma H_1 M_{oB} - \frac{i\gamma H_1 M_{oA}}{\alpha_A \tau_A + 1})(\tau_B)(\alpha_A \tau_A + 1)\right] /$$

$$\left[(\alpha_A \tau_A + 1)(\alpha_B \tau_B + 1) - 1\right] \qquad (45)$$

using

$$p_A = \tau_A/\tau_A + \tau_B, \quad p_B = \tau_B/\tau_A + \tau_B$$

$$p_A M_o = M_{oA} \qquad p_B M_o = M_{oB}$$

$$G = -i\gamma H_1 M_o \left[(p_A + \frac{p_B}{\alpha_B \tau_B + 1})(\tau_A)(\alpha_B \tau_B + 1) + \right.$$

$$\left.(p_B + \frac{p_A}{\alpha_A \tau_A + 1})(\tau_B)(\alpha_A \tau_A + 1)\right] / \left[(\alpha_A \tau_A + 1)(\alpha_B \tau_B + 1)\right] - 1 \qquad (46)$$

$$G = -i\gamma H_1 M_o \left[(p_A \alpha_B \tau_B + p_B + p_A)\tau_A + \right.$$

$$\left. p_B \alpha_A \tau_A + p_A + p_B)\tau_B\right] / \left[(\alpha_A \tau_A + 1)(\alpha_B \tau_B + 1) - 1\right] \qquad (47)$$

with $p_A + p_B = 1$

$$G = -i\gamma H_1 M_o \left[(p_A \alpha_B \tau_B \tau_A + \tau_A + p_B \alpha_A \tau_A \tau_B + \tau_B)\right] /$$

$$\left[(\alpha_A \tau_A + 1)(\alpha_B \tau_B + 1) - 1\right] \qquad (48)$$

or

$$G = -i\gamma H_1 M_o \left[(\tau_A + \tau_B) + \tau_A\tau_B(\alpha_A p_B + \alpha_B p_A)\right] /$$

$$\left[(\alpha_A\tau_A + 1)(\alpha_B\tau_B + 1) - 1\right] \qquad (49)$$

as obtained first by Gutowsky, McCall and Slichter (126). We must now separate the imaginary part from the real in Equation (49)

Define $\tau = \tau_A\tau_B/\tau_A + \tau_B$

Therefore $\tau_A = \tau/p_B$ and $\tau_B = \tau/p_A$

$$\text{let } Y = \frac{G}{-i\gamma H_1 M_o} = \frac{\tau_A + \tau_B + \tau_A\tau_B(\alpha_A p_B + \alpha_B p_A)}{\alpha_A\alpha_B\tau_A\tau_B + 1 + \alpha_B\tau_B + \alpha_A\tau_A - 1} \qquad (50)$$

dividing numerator and denominator by $\tau_A + \tau_B$

$$Y = \frac{\frac{\tau_A}{\tau_A + \tau_B} + \frac{\tau_B}{\tau_A + \tau_B} + \frac{\tau_A\tau_B}{\tau_A + \tau_B}(\alpha_A p_B + \alpha_B p_A)}{\frac{\tau_A\tau_B}{\tau_A + \tau_B}\alpha_A\alpha_B + \frac{\tau_B}{\tau_A + \tau_B}\alpha_B + \frac{\tau_A}{\tau_A + \tau_B}\alpha_A} \qquad (51)$$

$$\text{let } k_A = \frac{1}{T_{2A}}, \qquad k_B = \frac{1}{T_{2B}}$$

$\alpha_A = k_A - i(\omega_a - \omega)$ and $\alpha_A p_A = k_A p_A - i p_A(\omega_A - \omega)$

$$Y = 1 + \tau p_B(k_A - i(\omega_A - \omega)) + p_A(k_B - i\ (\omega_B - \omega\omega))/$$

$$\left[p_A(k_A - i(\omega_A - \omega))\right] + \left[(k_B - i(\omega_B - \omega))p_B\right] +$$

$$\left[k_A k_B - i(k_B(\omega_A - \omega) + (\omega_B - \omega)k_A) -\right.$$

$$\left.(\omega_A - \omega)(\omega_B - \omega)\right]\tau \qquad (52)$$

$$Y = 1 + \tau p_B k_A + p_A k_B - i\tau(p_B(\omega_A - \omega)$$

$$+ p_A(\omega_B - \omega))/p_A k_A + p_B k_B +$$

$$\tau\left[k_A k_B - (\omega_A - \omega)(\omega_B - \omega)\right] -$$

$$i\left[\tau k_B(\omega_A - \omega) + k_A(\omega_B - \omega) +\right.$$

$$\left.p_A(\omega_A - \omega) + p_B(\omega_B - \omega)\right] \qquad (53)$$

Let $S = p_A k_A + p_B k_B + \tau\left[k_A k_B - (\omega_A - \omega)(\omega_B - \omega)\right]$

$$T = (p_A + k_B)(\omega_A - \omega) + \tau(p_B + k_A)(\omega_B - \omega)$$

$$U = 1 + \tau p_B k_A + p_A k_B$$

$$V = \tau\left[p_B(\omega_A - \omega) + p_A(\omega_B - \omega)\right]$$

$$Y = \frac{U - iV}{S - iT} = \frac{(U - iV)(S + iT)}{S^2 + T^2} \qquad (54)$$

$$Y = \frac{SU + TV + i(UT - SV)}{S^2 + T^2} \tag{55}$$

$$G = - i\gamma H_1 M_o Y \tag{56}$$

$$G = - \gamma H_1 M_o \left(i \frac{SU + TV}{S^2 + T^2} + \frac{UT - SV}{S^2 + T^2} \right) \tag{57}$$

Since $G = u + iv$ (58)

$$u = - \gamma H_1 M_o \left[\frac{UT - SV}{S^2 + T^2} \right] \tag{59}$$

$$v = - \gamma H_1 M_o \left[\frac{SU + TV}{S^2 + T^2} \right] \tag{60}$$

where

$$S = \frac{P_A}{T_{2A}} + \frac{P_B}{T_{2B}} + \frac{\tau}{P_A P_B} \left(\frac{P_A P_B}{T_{2A} T_{2B}} - P_A P_B (\omega_A - \omega)(\omega_B - \omega) \right) \tag{61}$$

$$S = \frac{P_A}{T_{2A}} + \frac{P_B}{T_{2B}} + \frac{\tau}{T_{2A} T_{2B}} - \tau (\omega_A - \omega)(\omega_B - \omega) \tag{62}$$

$$U = 1 + \tau \left(\frac{P_B}{T_{2A}} + \frac{P_A}{T_{2B}} \right) \tag{63}$$

$$T = P_A(\omega_A - \omega) + P_B(\omega_B - \omega) + \tau \frac{(\omega_A - \omega)}{T_{2B}} + \tau \frac{(\omega_B - \omega)}{T_{2A}} \tag{64}$$

$$T = P_A\omega_A + P_B\omega_B - \omega(P_A + P_B) + \tau \left(\frac{\omega_A - \omega}{T_{2B}} + \frac{\omega_B - \omega}{T_{2A}} \right) \tag{65}$$

$$T = (P_A\omega_A + P_B\omega_B - \omega) + \tau \left(\frac{\omega_A - \omega}{T_{2B}} + \frac{\omega_B - \omega}{T_{2A}} \right) \tag{66}$$

$$V = (p_B\omega_A + p_A\omega_B - \omega) \tag{67}$$

In Summary

$$G = u + iv \tag{68}$$

$$u = -\gamma H_1 M_o \left(\frac{UT - SV}{S^2 + T^2}\right) \tag{69}$$

$$v = -\gamma H_1 M_o \left(\frac{SU + TV}{S^2 + T^2}\right) \tag{70}$$

$$S = \frac{p_A}{T_{2A}} + \frac{p_B}{T_{2B}} + \frac{\tau}{T_{2A}T_{2B}} - \tau(\omega_A - \omega)(\omega_B - \omega) \tag{71}$$

$$T = p_A\omega_A + p_B\omega_B - \omega + \tau\left(\frac{\omega_A - \omega}{T_{2B}} + \frac{\omega_B - \omega}{T_{2A}}\right) \tag{72}$$

$$U = 1 + \tau\left(\frac{p_B}{T_{2A}} + \frac{p_A}{T_{2B}}\right) \tag{73}$$

$$V = \tau(p_B\omega_A + p_A\omega_B - \omega) \tag{74}$$

Relation to a Complexation Equilibrium

Let's consider the following equilibrium

$$M + L \underset{k_b}{\overset{k_f}{\rightleftharpoons}} ML \tag{75}$$

where M is the observable nucleus which can be found, under certain circumstances in both sites M and ML the complex formation constant K is

$$K = \frac{C_{ML}}{C_M C_L} = \frac{k_f}{f_b} \tag{76}$$

In general the relaxation time is given by (127a)

$$\frac{1}{\tau_i} = \frac{\text{rate of removal of molecule from } i^{th} \text{ state, by exchange}}{\text{number of molecules in the } i^{th} \text{ state}} \tag{77}$$

then

$$\frac{1}{\tau_B} = \frac{\partial ML/\partial t}{C_{ML}} \tag{78}$$

$$\frac{1}{\tau_A} = \frac{\partial M/\partial t}{C_M} \tag{79}$$

$$\frac{\partial ML}{\partial t} = k_b \, C_{ML} \tag{80}$$

$$\frac{\partial M}{\partial t} = -k_f \, C_M \, C_L \tag{81}$$

Therefore

$$\frac{1}{\tau_B} = k_b \tag{82}$$

$$\frac{1}{\tau_A} = -k_f \, C_L \tag{83}$$

$$\tau = \tau_A \tau_B / \tau_A + \tau_B$$

$$p_A = \tau_A / \tau_A + \tau_B$$

$$p_B = \tau_B / \tau_A + \tau_B$$

then

$$\tau = p_A\tau_B = p_B\tau_A$$

with (83)

$$\tau = \frac{p_A}{k_b} \tag{84}$$

For equal population case $p_A = p_B = 0.5$ (84) becomes

$$\tau = \frac{1}{2k_b} \tag{85}$$

Therefore, from the value of τ at a given temperature, k_b can be obtained with (84). Thermodynamic parameters can then be calculated from the following equations (127b)

$$\left(\frac{\partial \ell nk}{\partial T}\right)_{v \text{ or } P} = E_a/RT^2 \tag{86}$$

$$\Delta H^{o\ddagger} = E_a - RT \tag{87}$$

$$\Delta S_o^{\ddagger} = R\ell n\, k_b - R\, \ell n\frac{KT}{h} + \Delta H_o^{\ddagger} \tag{88}$$

$$\Delta G_o^{\ddagger} = \Delta H_o^{\ddagger} - T\Delta S_o^{\ddagger} \tag{89}$$

where $\Delta G_o^{\ddagger}$, $\Delta H_o^{\ddagger}$ and $\Delta S_o^{\ddagger}$ are the standard free energy of activation, the standard enthalpy of activation and the standard entropy of activation respectively.

E_a is the Arrhenius activation energy

T the absolute temperature

h the Plank's constant

K the Bolzman's constant

B. Determination of τ Values from Line Shape Analysis of an NMR Spectrum at a Given Temperature. Description of Computer Program and Subroutine Equation.

The lineshape is a mixture of the absorption (v) and dispersion (u) components

$$V = u\sin\theta + v\cos\theta + c \qquad (90)$$

u and v are defined in Equations (69) and (70), respectively. The KINFIT program is used as described in Appendix II with the following parameters

NCST = 6 (number of constants)

CONST (1) = P_A

CONST (2) = P_B

CONST (3) = T_{2A}

CONST (4) - T_{2B}

CONST (5) = $\omega_A/2\pi$

CONST (6) = $\omega_B/2\pi$

NOVAR = 2 (number of variables)

XX (1) = $\omega/2\pi$

XX (2) = V

Each spectrum is fitted to four parameters (NOUNK = 4)

U (1) = normalization factor

U (2) = τ

U (3) = c (base line adjustment)

U (4) = θ

C. Determination of the Activation Energy (E_a). Description of the Computer Program and Subroutine Equation.

The Arrhenius activation energy (E_a) is given by

$$\left(\frac{\partial \ell nk}{\partial T}\right)_{v \text{ or } p} = E_a/RT^2 \tag{91}$$

or

$$k = k_{ref}\, e^{-\frac{E_a}{R}\left(\frac{1}{T} - \frac{1}{T_{ref}}\right)} \tag{92}$$

where T_{ref} is a reference temperature to which k_{ref} corresponds, and

$R = 1.987$ cal. mole^{-1} ^{o}K.

KINFIT program is used with

NCST = 2 (number of constants)

CONST (1) = R

CONST (2) = T_{ref}

```
FTN,
ATTACH(KINFIT,KINFIT)
LOAD(KINFIT)
LGO.
0000000000000000000000
      SUBROUTINE FON                                                    FON 1281
      COMMON KOUNT,ITAPE,JTAPE,IWT,LAP,XINCR,NOPT,NOVAR,NOUNK,XMIN,ITMAX,FON 1282
     1WTX,TEST,I,AV,NESTO,IAR,EPS,ITYP,XX,RXTYP,DX11,FOP,FO,FU,P,ZL,TA,FON 1283
     2TGVAL,XST,T,DT,L,M,JJJ,Y,DY,VECT,NCST,CONST
      DIMENSION X(4,100), U(20), WTX(4,100), XX(4), FOP(100), FO(100), FON 1285
     1U(100), P(20,21), VECT(20,21), ZL(100), TO(20), EIGVAL(20), XST(10FON 1286
     20), Y(10), DY(10), CONST(16)                                      FON 1287
      GO TO (2,3,4,5,1), ITYP
    1 CONTINUE
      ITAPE=60                                                          FON 1300
      JTAPE=61
      WRITE (ITAPE,6)
    6 FORMAT(*7 LI NAR TEMPERATURE DEPENDENCE *)
      NOUNK=4
      NOVAR=2
      RETURN
    2 CONTINUE
      PI=2.*3.14159
      S=(CONST(1)/CONST(3))+(CONST(2)/CONST(4))+U(2)/(CONST(3)*CONST(4))
     1-(PI*PI*U(2))*(CONST(5)-XX(1))*(CONST(6)-XX(1))
      Z=1.+U(2)*((CONST(2)/CONST(3))+(CONST(1)/CONST(4)))
      T=PI*((CONST(1)*CONST(5))+(CONST(2)*CONST(6))-XX(1))+(U(2)*PI)*(((
     1CONST(5)-XX(1))/CONST(4))+((CONST(6)-XX(1))/CONST(3)))
      V=U(2)*((CONST(2)*CONST(5))+(CONST(1)*CONST(6))-XX(1))*PI
      C=(U(1)*((S*T)+(Z*V)))/((S*S)+(T*T))+U(3))
      D=U(1)*((Z*T)-(S*V))/((S*S)+(T*T))
      E=SIN(U(4))*COS(U(4))*U(3)
      RESID=F-XX(2)
      RETURN                                                            FON 1332
    3 CONTINUE
      RETURN
    4 CONTINUE
      RETURN
    5 CONTINUE
      RETURN
      END
0000000000000000000000
     26          20                          6.0001
LIC(94,211), FORMAMIDEPA(I,1)=.65,PR(211)=.35,TEMP=149.3
.65          .35          .375         .375         31.00        21.30
59.0         .010         .05          .01
17.00        .01          0.00         .050         18.00        .01          0.10         .050
19.00        .01          0.25         .050         20.00        .01          0.60         .050
21.00        .01          0.90         .050         22.00        .01          1.25         .050
23.00        .01          1.50         .050         24.00        .01          1.55         .050
25.00        .01          1.55         .050         26.00        .01          1.60         .050
27.00        .01          1.75         .050         28.00        .01          2.15         .050
28.50        .01          2.40         .050         29.00        .01          2.65         .050
29.50        .01          2.95         .050         30.00        .01          3.20         .050
30.50        .01          3.30         .050         31.00        .01          3.20         .050
31.50        .01          2.95         .050         32.00        .01          2.40         .050
32.50        .01          1.80         .050         33.00        .01          1.30         .050
34.00        .01          0.50         .050         35.00        .01          0.20         .050
36.00        .01          0.19         .050         37.00        .01          0.00         .050
0000000000000000000000
0000000000000000005000
```

NOVAR = 2 (number of variables)

XX (1) = T

XX (2) = k

And NOUNK = 2 (number of parameters)

U (1) = k_{ref}

U (2) = E_a

```
FTN,
ATTACH(KINFIT,KINFIT)
LOAD(KINFIT)
LGO.
0000000000000000000000
      SUBROUTINE FON                                                    FON 1281
      COMMON KOUNT,ITAPE,JTAPE,IWT,LAP,XINCR,NOPT,NOVAR,NOUNK,X,U,ITMAX,FON 1282
     1WTX,TEST,T,AV,RESTO,IAP,EPS,ITYP,XX,RXTYP,DXII,FOP,FO,FU,P,ZL,TO,EFON 1283
     2IGVAL,XST,T,DT,L,W,JJ,Y,DY,VECT,NCST,CONST
      DIMENSION X(4,100), U(20), WTX(4,100), XX(4), FOP(100), FO(100), FFON 1285
     1U(100), P(20,21), VECT(20,21), ZL(100), TO(20), EIGVAL(20), XST(10FON 1286
     20), Y(10), DY(10), CONST(16)                                      FON 1287
      GO TO (2,3,4,5,1), ITYP
    1 CONTINUE                                                          FON 1296
      ITAPE=60                                                          FON 1300
      JTAPE=61
      WRITE (JTAPE,6)
    6 FORMAT(27 LI NMR ACTIVATION ENERGY *)
      NOUNK=2
      NOVAR=2
      RETURN
    2 CONTINUE
      C=U(1)*EXP(-(U(2)/CONST(1))*((1./XX(1))-(1./CONST(2))))
      RESID=C-XX(2)
      RETURN                                                            FON 1332
    3 CONTINUE
      RETURN
    4 CONTINUE
      RETURN
    5 CONTINUE
      RETURN
      END
0000000000000000000000
    7         20                    2.0001
LTCL04,211,BYRDINE ACTIVATION ENERGY
1.987      135.6
15.719     20000.0
335.6      .025        15.719    2.43       343.1     .025       27.610    5.36
399.6      .025        249.243   251.42     407.6     .025       632.044   1479.5
424.5      .025        1251.133  11452.75   432.4     .025       1533.315  9211.79
415.7      .025        333.207   3033.35
0000000000000000000000
0000000000000000000000
```

LITERATURE CITED

LITERATURE CITED

(1) D. N. Bhattacharyya, C. L. Lee, J. Smid and M. Szwarc J. Phys. Chem., 69, 608 (1965).

(2) C. Carvajal, K. J. Tölle, J. Smid and M. Szwarc, J. Amer. Chem. Soc., 87, 5548 (1965).

(3) Lydia G. Savedoff, J. Amer. Chem. Soc., 88, 664 (1966).

(4) Jurgen, H. Exner and Edwin C. Steiner, J. Amer. Chem. Soc., 96, 1782 (1974).

(5) P. Jagodzinski and S. Petrucci, J. Phys. Chem.,78, 917 (1974).

(6) J. C. Evans and G. Y. S. Lo, J. Phys. Chem., 69, 3323 (1965).

(7) W. F. Edgell, A. T. Watts, J. Lyford and W. M. Risen, Jr., J. Amer. Chem. Soc., 88, 1815 (1966).

(8) W. F. Edgell, A. Lyford, IV, R. Wright, W. M. Risen, Jr., and A. Watts, J. Amer. Chem. Soc., 92, 2240 (1970).

(9) B. W. Maxey and A. I. Popov, J. Amer. Chem. Soc., 89, 2230 (1967).

(10) B. W. Maxey and A. I. Popov, J. Amer. Chem. Soc., 91, 4352 (1969).

(11) B. W. Maxey and A. I. Popov, J. Amer. Chem. Soc. 91, 4352 (1969).

(12) J. L. Wuepper and A. I. Popov, J. Amer. Chem. Soc., 92, 1493 (1970).

(13) M. K. Wong, W. J. Mckinney and A. I. Popov, J. Phys. Chem., 75, 56 (1971).

(14) M. K. Wong and A. I. Popov, J. Inorg. Nucl. Chem., 33, 1203 (1971).

(15) W. J. Mckinney and A. I. Popov, J. Phys. Chem., 74, 535 (1970).

(16) P. R. Handy and A. I. Popov, Spectrochim. Acta., 28A, 1545 (1972).

(17) M. S. Greenberg, D. M. Wied and A. I. Popov, Spectrochim. Acta., 29A, 1927 (1973).

(18) A. T. Tstatsas and W. M. Risen, Jr., Chem. Phys. Lett., 7, 354 (1970).

(19) W. F. Edgell, W. R. Robinson, A. Barbetta and D. P. Schussler, J. Amer. Chem. Soc., 96, 415 (1974).

(20) J. Barriol, P. Bonnet and J. Devaure, J. Chim. Phys., 71, 107 (1974).

(21) A. Regis, J. Corset, J. Chim. Phys. Physico. Chim. Biol., 69, 1508 (1972).

(22) A. Regis, J. Corset, Can. J. Chem., 51, 3577 (1973).

(23) R. G. Baum and A. I. Popov, to be published.

(24) B. W. Maxey and A. I. Popov, J. Amer. Chem. Soc., 90, 4470 (1968).

(25) E. Schaschel, M. C. Day, J. Amer. Chem. Soc., 10, 503 (1968).

(26) A. Fratiello, R. E. Lee, D. P. Miller and V. M. Nishida, Mol. Phys., 10, 551 (1966).

(27) R. P. Taylor and I. D. Kuntz, Jr., J. Amer. Chem. Soc., 92, 4815 (1970).

(28) C. Deverell and R. E. Richards, Mol. Phys., 10, 551 (1966).

(29) Edwin D. Becker, Appl. Spectrosc., 26, 421 (1972).

(30) Daniel A. Netzel, Appl. Spectrosc., 26, 430 (1972).

(31) C. J. Jameson and H. S. Gutowsky, J. Chem. Phys., 40, 1714 (1964).

(32) R. H. Erlich, E. Roach, A. I. Popov, J. Amer. Chem. Soc., 92, 4989 (1970).

(33) M. Herlem and A. I. Popov, J. Amer. Chem. Soc., 94, 1431 (1972).

(34) R. H. Erlich and A. I. Popov, J. Amer. Chem. Soc., 93, 5260 (1971).

(35) M. S. Greenberg, R. L. Bodner and A. I. Popov, J. Phys. Chem., 77, 2449 (1973).

(36) R. H. Erlich, M. S. Greenberg and A. I. Popov, Spectrochim. Acta., in press.

(37) G. J. Templeman and A. L. VanGeet, J. Amer. Chem. Soc., 94, 5578 (1972).

(38) a) V. Gutmann and E. Wychera, Inorg. Nucl. Chem. Lett., 2, 257 (1966).

b) V. Gutmann, "Coordination Chemistry in Nonaqueous Solvents" Springer-Verlag, Vienna (1968).

(39) M. S. Greenberg, Ph.D. Thesis, Michigan State University, East Lansing, Michigan (1974).

(40) A. L. Van Geet, J. Amer. Chem. Soc., 94, 5583 (1972).

(41) J. W. Akitt and A. J. Downs, "The Alkali Metals" International Symposium held at Nottingham, July 19-22, 1966, Special Pub. No. 22, The Chem. Soc., Burlington House, London (1967).

(42) A. Attalla and R. R. Eckstein, Anal. Chem., 43, 949 (1971).

(43) R. A. Craig and R. E. Richards, Trans. Faraday. Soc., 59, 1972 (1963).

(44) G. E. Maciel, J. K. Hancock, L. F. Lafferty, P. A. Mueller and W. K. Musker, Inorg. Chem., 5, 554 (1966).

(45) R. H. Cox, H. W. Terry, Jr., Lester W. Harrison, J. Amer. Chem. Soc., 93, 3297 (1971).

(46) R. H. Cox, H. W. Terry, Jr., J. Magn. Reson., 14, 317 (1974).

(47) E. T. Roach, P. R. Handy and A. I. Popov, Inorg. Nucl. Chem. Lett., 9, 359 (1973).

(48) R. L. Bodner, M. S. Greenberg, and A. I. Popov, Spectrosc. Lett., 5, 489 (1972).

(49) P. R. Handy, Ph.D. Thesis, Michigan State University East Lansing, Michigan (1972).

(50) K. J. Johnson, J. P. Hunt and H. W. Dodgen, J. Chem. Phys., 51, 4993 (1969).

(51) Yasukazu Saito, Can. J. Chem., 43, 2532 (1965).

(52) C. Hall, G. L. Haller and R. E. Richards, Mol. Phys., 16, 377 (1969).

(53) C. H. Langford and T. R. Stengle, J. Amer. Chem. Soc., 91, 4014 (1969).

(54) C. Deverell and R. E. Richards, Mol. Phys., 16, 421 (1969).

(55) C. Hall, "The Application of Chlorine, Bromine and Iodine N.M.R. Spectroscopy to the Study of Physico-Chemical Processes in Liquids", Quart. Rev., 25, 87 (1971).

(56) J. P, K. Tong and C. H. Langford, Can. J. Chem., 52, 1721 (1974).

(57) E. G. Gross and R. M. Featherstone, J. Pharmacol. Exp. Therap., 87, 291 (1946).

(58) W. E. Stone, Pharmacology, 3, 367 (1970).

(59) F. M. D'Itri and A. I. Popov, J. Amer. Chem. Soc., 90, 6476 (1968).

(60) R. M. Izatt, J. H. Rytting, D. P. Nelson, B. L. Haymore, J. J. Christensen, Science, 164, 443 (1969).

(61) C. J. Pedersen, J. Amer. Chem. Soc., 89, 7017 (1967).

(62) M. A. Bush and M. R. Truter, J. Chem. Soc., 341 and 345 (1972).

(63) P. R. Mallinson and M. R. Truter, J. Chem. Soc., 1818 (1972).

(64) J. L. Dye, M. G. DeBacker, V. A. Nicely, J. Amer. Chem. Soc., 92, 5226 (1970).

(65) C. J. Pedersen, J. Amer. Chem. Soc., 92, 5226 (1970).

(66) Ibid, 92, 391 (1970).

(67) H. K. Frensdorff, J. Amer. Chem. Soc., 93, 600 (1971).

(68) Ibid, 93, 4684 (1971).

(69). A. T. Tsatsas, R. W. Stearns and W. M. Risen, J. Amer. Chem. Soc., 94, 5247 (1972).

(70) E. Shchori, J. Jagur-Grodzinski, Z. Luz and M. Shporer, J. Amer. Chem. Soc., 93, 7133 (1971).

(71) K. H. Wong, G. Konizer and J. Smid, J. Amer. Chem. Soc., 92, 666 (1970).

(72) C. J. Pedersen and H. K. Frensdorff, Angew. Chem. 11, 16 (1972).

(73) S. Kopolow, Z. Macharek, U. Takaki and J. Smid, J. Macromol. Sci. Chem., A7(5), 1015 (1973).

(74) P. B. Chock, Proc. Nat. Acad. Sci. US, 69, 1939 (1972)

(75) D. F. Evans. S. L. Wellington, J. A. Nadis and E. L. Cussler, J. Solut. Chem. 1, 499 (1972).

(76) Sam. D. J. and H. Simmons, J. Amer. Chem. Soc., 96, 2250 (1974).

(77) B. Dietrich, J. M. Lehn and J. P. Sauvage, Tetrahedron Lett., 2885 and 2889 (1969).

(78) B. Dietrich, J. M. Lehn and J. P. Sauvage, and J. Blanzat, Tetrahedron 29, 1629 (1973).

(79) W. E. Morf and W. Simon, Helv. Chim. Acta., 54, 2683 (1971).

(80) J. M. Lehn "Design of Organic Complexing Agents" Structure and Bonding, 16, 1 (1973).

(81) J. M. Ceraso, J. L. Dye, J. Org. Chem., 38, 1773 (1973).

(82) Roland Wiest and Raymond Weiss, J. Chem. Soc. Chem., Commun, 678 (1973).

(83) D. Moras, B. Metz and R. Weiss, Acta. Crystallogr., B29, 388 (1973).

(84) Ibid, B29, 383 (1973).

(85) D. Moras and R. Weiss, Acta. Crystallogr., B29, 396 (1973).

(86) Ibid, B29, 400 (1973).

(87) C. H. Park, H. E. Simmons, J. Amer. Chem. Soc., 94, 7184 (1972).

(88) H. E. Simmons, C. H. Park, J. Amer. Chem. Soc., 90, 2428 (1968).

(89) C. H. Park, H. E. Simmons, J. Amer. Chem. Soc., 90, 2429 (1968).

(90) J. M. Lehn and J. P. Sauvage, Chem. Commun, 440 (1971).

(91) J. Cheney and J. M. Lehn, J. Chem. Soc. Chem. Commun., 487 (1972).

(92) J. Cheney, J. M. Lehn, J. P. Sauvage and M. E. Stubbs, J. Chem. Soc. Chem. Commun., 1100 (1972).

(93) J.M. Lehn and F. Montavon, Tetrahedron Lett. 44, 4557 (1972).

(94) B. Dietrich, J. M. Lehn and J. P. Sauvage, J. Chem. Soc. Chem. Commun., 15 (1973).

(95) W. E. Morf and W. Simon, Hel. Chim. Acta., 54, 2683 (1971).

(96) J. J. Christensen, D. J. Eatough and R. M. Izatt, Chem. Rev., 74, 351, 384 (1974).

(97) J. M. Lehn, J. P. Sauvage, B. Dietrich, J. Amer. Chem. Soc., 92, 2916 (1970).

(98) J. M. Ceraso, J. L. Dye, J. Amer. Chem. Soc., 95, 4432 (1973).

(99) J. P. Kintizinger, J. M. Lehn, J. Amer. Chem. Soc., 96, 3313 (1974).

(100) J. L. Dye, "Metal Solutions in Amines and Ethers". Electrons in Fluids p. 77-95, Springer-Verlay, Berlin, Heidelberg, New York (1973).

(101) J. L. Dye, Mei Tak Lok, F. J. Tehan, R. B. Coolen, N. Papadakis, J. M. Ceraso and M. G. Debacker, Verlag Chemie GmbH, Weinheim/Bergstr Band., 75 Heft 7 (1971).

(102) Mei Tak Lok, F. J. Tehan and J. L. Dye, J. Phys. Chem., 76, 2975 (1972).

(103) J. L. Dye, J. M. Ceraso, Mei Tak Lok, B. L. Barnett, F. J. Tehan, J. Amer. Chem. Soc., 96, 608 (1974).

(104) F. J. Tehan, B. L. Barnett, J. L. Dye, J. Amer. Chem. Soc., 96, 7203 (1974).

(105) J. M. Ceraso and J. L. Dye, J. Chem. Phys., 61, 1585 (1974).

(106) G. Foex, C. J. Gorter and L. J. Smits, "Constantes Selectionnees, Diamagnetisme et Paramagnetisme, Relaxation Paramagnetique" Masson & Cie Editeurs, Paris (1957).

(107) D. H. Live and S. I. Chan, Anal. Chem., 42, 791 (1971).

(108) J. L. Dye and V. A. Nicely, J. Chem. Educ. 48, 443 (1968).

(109) E. G. Bloor and R. G. Kidd, Can. J. Chem., 46, 3425 (1968).

(110) A. I. Popov and N. E. Skelly, J. Amer. Chem. Soc., 76, 5309 (1954).

(111) U. Mayer and V. Gutmann, Structure and Bonding 12, 113 (1972).

(112) N. A. Matwiyoff and H. Taube, J. Amer. Chem. Soc., 90, 2796 (1972).

(113) A. P. Zipp, J. Phys. Chem., 78, 556 (1974).

(114) T. C. Farrar and E. D. Becker "Pulse and Fourier Transform NMR", Academic Press, New York, 1971, Chapter IV.

(115) A. Abragam, "The Principles of Nuclear Magnetic Resonance", Oxford University Press, London, 1951 p. 313 ff.

(116) M. St. J. Arnold and K. J. Packer, Mol. Phys., 14, 241 (1968).

(117) T. E. Burke and S. I. Chan, J. Mag. Resonance, 3, 55 (1970).

(118) T. R. Stengle, Personal communication.

(119) Unpublished work, this laboratory.

(120) J. M. Lehn and J. P. Sauvage, Paper presented at conference Thermodynamique Chimique, Societe Chimique de France, Bordeaux, France, October 20, 1972.

(121) E. Shchori, J. J. Grodzinski and M. Shporer, J. Amer. Chem. Soc., 95, 3842 (1973).

(122) J. A. Pople, W. G. Schneider and H. J. Bernstein, "High Resolution Nuclear Magnetic Resonance": McGraw Hill Book Co., New York, NY, 1959, p. 218-224. An error in their equation (10-14) in which p_A and p_B are interchanged was propagated in Reference (98). In the latter case p_A and p_B were equal so the error did not affect the final results.

(123) W. E. Wentworth, J. Chem. Educ., 42, 96 (1965).

(124) K. J. Laider, "Chemical Kinetics", McGraw Hill Book Co., New York, NY, 1965, p. 251-253.

(125) H. M. McConnell, J. Chem. Phys., 28, 430 (1958).

(126) H. S. Gutowsky, D. W. McCall and C. P. Shichter, Phys. Rev., 84, 589 (1951).

(127) Amdur and Hammes. "Chemical Kinetics Principles and Selected Topics", McGraw Hill Book Co., New York, NY, 1966, a) p. 147; b) p. 53-55.

MICHIGAN STATE UNIVERSITY LIBRARIES
3 1293 03082 4258